
SMART SAMPLING: HELPING FROM FRIENDLY NEIGHBORS FOR DECENTRALIZED FEDERATED LEARNING

Lin Wang¹, Yang Chen¹, Yongxin Guo¹, Xiaoying Tang¹

¹School of Science and Engineering, The Chinese University of Hong Kong (Shenzhen).

Abstract

Federated Learning (FL) is gaining widespread interest for its ability to share knowledge while preserving privacy and reducing communication costs. Unlike Centralized FL, Decentralized FL (DFL) employs a network architecture that eliminates the need for a central server, allowing direct communication among clients and leading to significant communication resource savings. However, due to data heterogeneity, not all neighboring nodes contribute to enhancing the local client’s model performance. In this work, we introduce *AFIND+*, a simple yet efficient algorithm for sampling and aggregating neighbors in DFL, with the aim of leveraging collaboration to improve clients’ model performance. *AFIND+* identifies helpful neighbors, adaptively adjusts the number of selected neighbors, and strategically aggregates the sampled neighbors’ models based on their contributions. Numerical results on real-world datasets with diverse data partitions demonstrate that *AFIND+* outperforms other sampling algorithms in DFL and is compatible with most existing DFL optimization algorithms.

1 Introduction

Federated Learning (FL), a collaborative machine learning paradigm, has garnered attention for its capacity to train models on decentralized devices without sharing raw data [1]. This method addresses privacy and communication concerns, proving valuable in fields like healthcare [2], energy [3], and manufacturing [4]. In Centralized FL (CFL), a central server selects clients for training, where effective client sampling is key for accelerating convergence and reducing communication overhead [5, 6, 7]. However, due to data heterogeneity among clients, it’s challenging to attain satisfactory performance for all using a single average central model [8, 9].

In contrast, decentralized federated learning (DFL), illustrated in Figure 1, utilizes a peer-to-peer structure where clients exchange model parameters directly, bypassing a central server [10]. Each client develops a local, personalized model, addressing the model shift caused by data heterogeneity in Centralized FL (CFL) [11, 12]. This shift to a decentralized architecture enhances privacy and reduces reliance on central infrastructure [13]. In particular, this decentralization does not need a global model explicitly or implicitly through the central server, thus significantly reducing the communication burden on the server side [14].

Despite its advantages, DFL encounters challenges due to network heterogeneity, affecting collaborative efficiency among clients [15]. Similar to CFL, selecting neighboring nodes¹ for collaboration is crucial in DFL as different collaborations resulting different model performance [16, 17]. We break down the neighbor node cooperation problem in DFL into three progressive challenges: identifying the right neighbors for collaboration, adaptively setting the number of participating clients, and valuing the importance of each selected client for aggregation.

Challenge 1: Identify the right neighbors for collaboration. Data heterogeneity across clients results in varied node distributions. Inappropriate neighbor selection can lead to performance degradation compared to solo training, while effective selection significantly boosts performance, as depicted in Fig 2. The underlying

¹The terms client, node, and neighbor are used interchangeably in this paper.

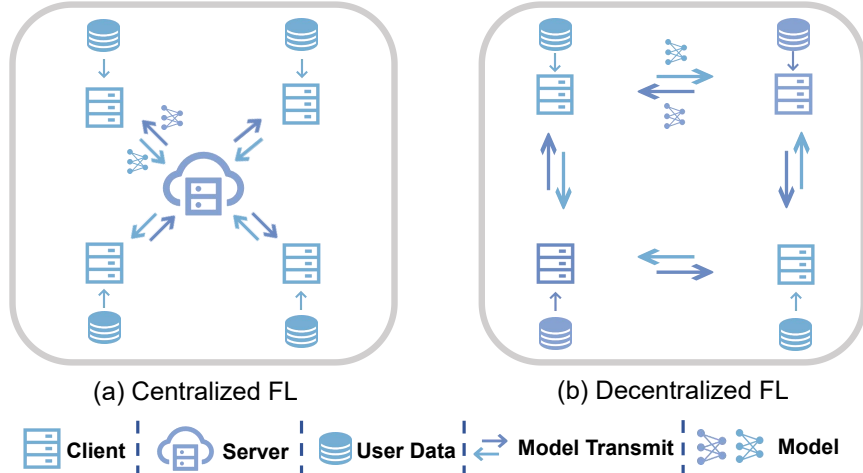


Figure 1: **Illustration of Centralized FL and Decentralized FL.** In centralized FL, communication takes place between the server and the clients, whereas in decentralized FL, it occurs directly between clients without the need for a central server.

principle is the similarity in data distribution between clients, such as between Client 1 and Client 2, as opposed to the divergent distribution of Client 3. This highlights the importance of similarity in client sampling. To understand how similarity aids in finding suitable collaborators theoretically, we explore the concept of a coreset for DFL client sampling, discussed in more detail in Section 3.2.

Challenge 2: Adaptive neighbor sampling. In addition to data heterogeneity, the number of sampled clients is crucial. Fixed-number sampling methods may perform poorly on new tasks without fine-tuning, which is resource-intensive and often ineffective [18]. For example, in Figure 2, setting the neighbor sampling number to 2 (involving Client 1, Client 2, and Client 3) worsens performance compared to collaboration between Client 1 and Client 2 alone. To address the limitations of fixed-number sampling, we propose a *participation threshold* to evaluate the overall similarity between a client and its neighbors. This threshold adjusts based on neighbor distribution similarity. A higher threshold is set when neighbors have diverse distributions, reducing the number of sampled clients to avoid those who negatively contribute. Conversely, a lower threshold is applied when most neighbors have similar distributions to the client.

Challenge 3: Aggregate the sampled clients. Current DFL client sampling algorithms, after selecting a subset of neighbors for collaboration, often overlook the aggregation step, typically averaging the models received from neighbors [19]. However, effective aggregation is crucial in FL to maximize the efficiency of sampling [6, 20]. The varying data distributions among sampled clients lead to differing contributions to collaboration. As shown in the experimental results of Figure 4, contribution-aware aggregation, which considers the individual impact of each client, is more effective than simple averaging, leading to faster convergence.

To this end, we propose **AFIND+**, an **A**daptive **Fr**riendly **N**eighbor **D**iscory algorithm, designed to enhance collaboration and performance of DFL. Specifically, based on theoretical and empirical observations, AFIND+ uses the output of a featurizer as a proxy for clients’ model similarity to identify neighbors with similar data distributions. To adaptively adjust the number of collaborators, AFIND+ sets a threshold to terminate the greedy selection process using confidence levels in client and neighbor similarity. Among the selected neighbors, AFIND+ assesses their importance to the client and reweights them for aggregation based on their contributions.

The contribution and novelty of AFIND+ can be summarized as follows:

- To the best of our knowledge, this work is the first to provide both theoretical insights and empirical evidence that, in DFL, helpful collaborators are those possessing similar data distributions. Based on this insight, we propose a greedy selection strategy to identify such collaborators.
- By proposing the use of the confidence level between clients and neighbors, it is the first to enable a dynamic number of collaboration neighbors, which helps set a termination for the greedy selection.



Figure 2: **Toy examples show the importance of appropriate cooperation.** Clients 1 and 2 have FashionMNIST datasets with labels $\{4, 5, 6, 7\}$, while Client 3’s dataset has labels $\{0, 1, 2, 3\}$. Using Client 2 as a baseline, accuracy comparisons indicate that collaboration between clients with similar data (Clients 1 and 2) is beneficial, whereas cooperation between clients with diverse data (Clients 2 and 3) is detrimental.

- It strategically aggregates the sampled neighbors based on their contributions, instead of merely sampling and leaving them alone, differing from existing methods.
- Theoretically, we provide convergence guarantees for our algorithm in a general nonconvex setting, achieving a convergence rate of $\mathcal{O}\left(\frac{1}{\sqrt{T}} + \frac{1}{T}\right)$. Empirically, we conduct extensive experiments on realistic data tasks using diverse data partition methods, evaluating the efficacy of our algorithm compared with the SOTA sampling baselines in DFL, achieving a maximum improvement of 5% on CIFAR-10 and 4% on CIFAR-100.

2 Related Works

DFL is a peer-to-peer communication learning paradigm, with clients connecting solely to their neighbors [21, 22, 23]. Neighbor selection has been shown to be an important challenge for DFL [18, 19, 24]. In this work, we address this challenge for DFL with a novel collaboration strategy AFIND+. A more comprehensive discussion of the related work can be found in Appendix A.

3 AFIND+: Adaptive Collaboration for DFL

In this section, we first define the problem setup and necessary notations for DFL. Then, we introduce AFIND+ (Algorithm 1), which includes finding the right neighbors via coreset (Sec 3.2), setting an adaptive participation threshold based on confidence levels (Sec 3.3), and contribution-based reweight aggregation (Sec 3.4).

3.1 Preliminary

Decentralized Federated Learning (DFL). In a standard DFL scenario with m clients, each client $i \in [m]$ possesses a local dataset D_i containing N_i data examples. The parameters of the model are denoted by $\mathbf{x} \in \mathbb{R}^d$, and $F_i(\mathbf{x}; \xi_i)$ represents the local objective function for client i , corresponding to the training samples ξ_i . The loss function for client i is given as $F_i(\mathbf{x}; \xi_i)$. The typical goal in DFL involves solving the following finite-sum stochastic optimization problem:

$$\min_{\mathbf{x}} f(\mathbf{x}) = \frac{1}{m} \sum_{i=1}^m F_i(\mathbf{x}; \xi_i). \quad (1)$$

In a decentralized network topology, client communication is represented by an undirected graph $\mathcal{G} = (\mathcal{N}, \mathcal{V}, \mathcal{W})$. Here, $\mathcal{N} = [1, \dots, m]$ denotes the set of clients, $\mathcal{V} \in \mathcal{N} \times \mathcal{N}$ signifies the set of communication channels connecting two distinct clients, and the connection matrix $\mathcal{W} = [w_{i,j}] \in [0, 1]^{m \times m}$ indicates the

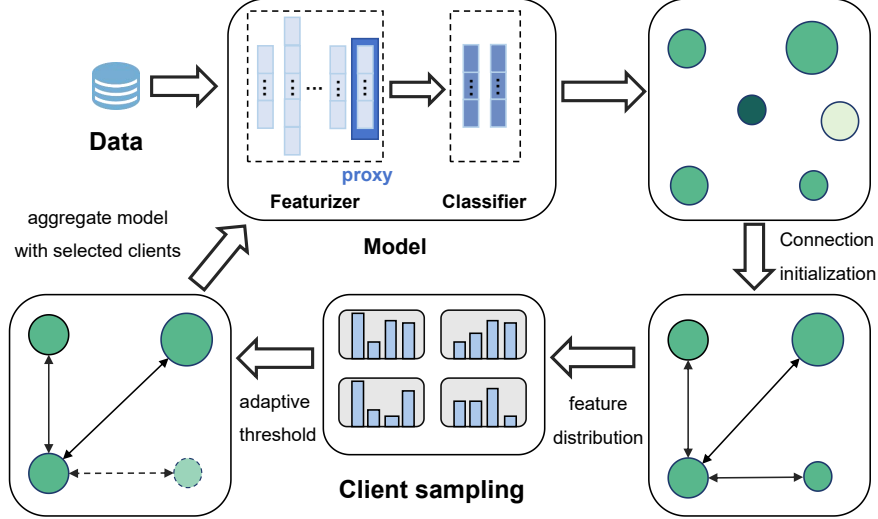


Figure 3: **Illustration of the AFIND+ method.** The node represents the clients in the network, with different sizes and colors indicating variations in data distribution. First, the client identifies helpful neighbors with similar data distribution, represented by a similar feature proxy. Next, it filters neighbors using a threshold based on overall distribution and helpfulness. Finally, it aggregates the selected clients based on their contributions.

presence of communication links between any two clients [25]. We define S_i as the set of nodes that can communicate with client i , where $w_{i,j} = 1$ for all $j \in S_i$.

DFL with personalized model. When considering a personalized model approach for DFL, the objective can be formulated as follows:

$$\min_{\mathbf{w}, \beta} \left\{ f(\mathbf{w}, \beta) := \frac{1}{m} \sum_{i=1}^m F_i(\mathbf{w}, \beta_i) \right\}, \quad (2)$$

where $\mathbf{w} \in \mathbb{R}^{d_0}$ represents the consensus model, averaged from all shared parameters \mathbf{w}_i , i.e., $\mathbf{w} = \frac{1}{m} \sum_{i=1}^m \mathbf{w}_i$, $\beta = (\beta_1, \dots, \beta_m)$ with $\beta_i \in \mathbb{R}^{d_i}$, $\forall i \in [m]$ corresponds to the local parameters, and $F_i(\mathbf{w}, \beta_i) = \mathbb{E}_{\xi_i \sim D_i} [F_i(\mathbf{w}, \beta_i; \xi_i)]$. Stochastic gradients with respect to \mathbf{w}_i and β_i are denoted as $\nabla_{\mathbf{w}}$ and ∇_{β} , respectively.

In DFL, the shared parameters \mathbf{w}_i of each client i are transmitted to their neighbors, denoted as S_i . Conversely, the personal parameters β_i only perform multiple local iterations in each client i and are not shared externally.

3.2 Identify Right Neighbors

In DFL, the goal is to find neighbors that improve a client’s performance, unlike CFL which aims to select a subset approximating full client participation [26]. Motivated by the effectiveness of selective collaboration shown in Figure 2, our focus is on identifying beneficial neighbors for each client.

We have posited that selecting the correct neighbors entails choosing those with similar data distributions, as depicted in Figure 2. A similar observation was made in [18]. We begin by analyzing the rationale behind this assertion from a theoretical standpoint, employing a coreset approach. Coresets are subsets of data points that effectively approximate the original dataset and are commonly utilized in active learning [27]. The coreset definition is as follows:

Definition 3.1 (Coreset). *Given a dataset \mathcal{D} and a loss function L , a coreset \mathcal{C} is a subset of \mathcal{D} such that for any model \mathbf{x} , the following inequality holds:*

$$\|L(\mathbf{x}, \mathcal{D}) - L(\mathbf{x}, \mathcal{C})\| \leq \epsilon, \quad (3)$$

where ϵ is a small error tolerance.

In DFL, the coreset of a target client is a set of clients that have similar model update performance. To formulate this problem, we start by following the logic in [28]. Let S be a subset of m clients. Furthermore, assume that there is a mapping $\varsigma_{\mathbf{x}} : V \rightarrow S$ that for every possible value of optimization parameter

$\mathbf{x} \in \mathcal{X}$ assigns every possible neighbor $i \in V$ to one of the elements j in S , i.e., $\varsigma_{\mathbf{x}}(i) = j \in S$. Let $C_j = \{i \in [m] \mid \varsigma(i) = j\} \subseteq V$ be the set of neighbors that are assigned to $j \in S$, and $\gamma_j = |C_j|$ be the number of such neighbor nodes. Hence, $\{C_j\}_{j=1}^m$ form a partition of V . Then, for any \mathbf{x} we can write the following gradient for client i :

$$\nabla F_i(\mathbf{x}) = \nabla F_i(\mathbf{x}) - \sum_{i \in V} \nabla F_i(\mathbf{x}) + \sum_{i \in V} (\nabla F_i(\mathbf{x}) - \nabla F_{\varsigma_{\mathbf{x}}(i)}(\mathbf{x}) + \nabla F_{\varsigma_{\mathbf{x}}(i)}(\mathbf{x})) \quad (4)$$

$$= \nabla F_i(\mathbf{x}) - \sum_{i \in V} \nabla F_i(\mathbf{x}) + \sum_{i \in V} [\nabla F_i(\mathbf{x}) - \nabla F_{\varsigma_{\mathbf{x}}(i)}(\mathbf{x})] + \sum_{j \in S} \gamma_j \nabla F_j(\mathbf{x}). \quad (5)$$

Subtracting, and then taking the norm of both sides, we get an upper bound on the error of estimating the client i 's gradient:

$$\|\nabla F_i(\mathbf{x}) - \sum_{j \in S} \gamma_j \nabla F_j(\mathbf{x})\|^2 \leq 2\|\nabla F_i(\mathbf{x}) - \sum_{i \in V} \nabla F_i(\mathbf{x})\|^2 + 2 \sum_{i \in V} \|\nabla F_i(\mathbf{x}) - \nabla F_{\varsigma_{\mathbf{x}}(i)}(\mathbf{x})\|^2, \quad (6)$$

where the inequality follows from the triangle inequality and Jensen's inequality. The upper bound in Eq. (6) is minimized when $\varsigma_{\mathbf{x}}$ assigns every $i \in V$ to an element in S with the most gradient similarity at parameter \mathbf{x} , or the minimum Euclidean distance between the gradient vectors at \mathbf{x} . Therefore, based on the above conclusion that helpful neighbors should be clients with the most gradient similarity, we can formally define the coreset of DFL as follows:

Definition 3.2 (Coreset of DFL). *Give a set of clients $[m]$ and loss function L , a coreset of client i in DFL is a subset of $[m]$ such that*

$$\sum_{j \in C_i^*} \|\nabla F_i(\mathbf{x}; D_i) - \nabla F_j(\mathbf{x}; D_j)\|^2 \leq \epsilon_i, \quad (7)$$

where C_i^* represents the coreset of client i , and ϵ_i represents the error tolerance of client i .

The definition of coreset in DFL implies that, within a defined tolerance error, the coreset of client i should be clients with similar model gradients. Motivated by the above theoretical findings and empirical observations (Figure 2 and [19]) — where a smaller distance among clients' data distribution (reflected in model distance) improves performance—we propose a greedy sampling approach to identify the helpful clients.

Clients with greater similarity in model gradients have a higher probability of being sampled. To reduce computation and communication costs, we use the output layer of the clients' featurizer as a feature proxy for the client's data distribution instead of the gradient for similarity calculation. It is worth noting that using the proxy does not cause additional information leakage compared to vanilla DFL approaches, as the proxy only constitutes one layer of the entire model. Specifically, the sampling probability for client j to be sampled by client i is calculated as:

$$p_{i,j}^t = \frac{\exp(\text{sim}(\phi_i^t, \phi_j^t)/v)}{\sum_{k \in \mathcal{B}_i^t} \exp(\text{sim}(\phi_i^t, \phi_k^t)/v)}, \quad (8)$$

where ϕ_i^t represents the feature proxy of client i at round t , and \mathcal{B}_i^t represents the available neighbors of client i at round t . Temperature v controls the distribution shape. The 'sim' refers to the cosine similarity between two vectors.

In practice, only a subset of clients are available in each round; thus, we let

$$p_{i,j}^t = \frac{\exp(\text{sim}(\phi_i^t, \phi_j^t)/v)}{\sum_{k \in C_i^t} \exp(\text{sim}(\phi_i^t, \phi_k^t)/v)} \left(1 - \sum_{i \in \mathcal{B}_i^t/C_i^t} p_{i,t}^t\right), \quad (9)$$

where C_i^t is the selected coreset for client i at round t and the multiplicative factor ensures that all probabilities sum to 1.

By $p_{i,j}^t$ we can identify helpful neighbors for client i , i.e., clients with a higher probability for collaboration. This is a greedy selection process. However, determining its termination conditions is challenging. To address this, we propose an adaptive threshold to control the number of participating clients, as detailed in the next section.

3.3 Adaptive Threshold for Flexible Neighbor Participation

We aim to select all helpful clients for collaboration in each round. However, as noted in **Challenge 2**, we don't know the number of helpful neighbors in each round. Simply fixing the number of collaborators can lead to poor performance, and fine-tuning this number during training is impractical.

Algorithm 1 AFIND+

Input: Number of clients m , global threshold τ , learning rate $\eta_{\mathbf{w}}$ and η_{β} , number of local epoch $K_{\mathbf{w}}$ and K_{β} , total training rounds T .

Output: Final model parameter \mathbf{w}_i^T and β_i^T

Initialize: Shared model \mathbf{w}_i^0 and personalized model β_i^0 . $p_{i,j} = \frac{1}{n_i}$ where $n_i = |\mathcal{B}_i^0|$ is the connected neighbors of client i , $\forall i \in [m]$.

```

1: for  $t = 0$  to  $T - 1$  do
2:   for client  $i$  in parallel do
3:     if  $p_{i,j}^t \geq \theta_i^t$ , for  $j$  in  $\mathcal{B}_i^t$  then
4:       Add neighbor  $j$  into the coreset  $C_i^t$  for collaboration
5:     end if
6:     for client  $j$  in  $C_i^t$  do
7:       Let  $\mathbf{w}_j^{t,0} = \mathbf{w}_i^t$ , calculate  $\phi_j^t \leftarrow [\nabla_{\mathbf{w}} F_j(\mathbf{w}_i^t, \beta_j^t; \xi_j)]_{\phi}$  and  $F_j(\mathbf{w}_i^t, \beta_j^t; \xi_j)$ ;
8:       Local Update  $\mathbf{w}_j$  and  $\beta_j$  and calculate  $\tilde{F}_j(\mathbf{w}_i^t, \beta_j^t; \xi_j)$  based on Eq. (15);
9:       Communicate  $\phi_j^t$ ,  $w_j^{t+1}$ , and  $\tilde{F}_j(\mathbf{w}_i^t, \beta_j^t; \xi_j)$  to client  $i$ 
10:    end for
11:     $\phi_i^t \leftarrow [\nabla_{\mathbf{w}} F_i(\mathbf{w}_i^t, \beta_i^t; \xi_i)]_{\phi}$ 
12:    Local Update  $\mathbf{w}_i$  and  $\beta_i$ ;
13:    Aggregation:  $\mathbf{w}_i^{t+1} = \sum_{j \in C_i^t} \varpi_{i,j}^t \mathbf{w}_j^{t+1}$ , where  $\varpi_{i,j}^t$  follows from Eq. (16);
14:    Update  $p_{i,j}^t$  and  $\theta_i^t$  based on Eq. (9) and Eq.(13), respectively;
15:  end for
16: end for

```

```

17:   /* Local Update w and beta */
18:   for  $k = 0$  to  $K_{\beta} - 1$  do
19:      $\beta_i^{t,k+1} = \beta_i^{t,k} - \eta_{\beta} \nabla_{\beta} F_i(\mathbf{w}_i^t, \beta_i^{t,k}; \xi_i)$ 
20:   end for
21:    $\beta_i^{t+1} \leftarrow \beta_i^{t,K_{\mathbf{w}}}$ 
22:   for  $k = 0$  to  $K_{\mathbf{w}} - 1$  do
23:      $\mathbf{w}_i^{t,k+1} = \mathbf{w}_i^{t,k} - \eta_{\mathbf{w}} \nabla_{\mathbf{w}} F_i(\mathbf{w}_i^{t,k}, \beta_i^{t+1}; \xi_i)$ 
24:   end for

```

To this end, we propose an adaptive threshold that assesses the overall distribution similarity between a client and all its available neighbors, updating as training progresses. Intuitively, if a client's neighbors tend to be more similar, the similarity threshold should adaptively decrease, allowing for a larger sampling pool. Conversely, if the neighbors are less similar to the client, the threshold should increase, potentially reducing the number of selected clients.

Motivated by the principles from GNN-FD [29], the threshold setting should correlate with the model's confidence in the overall similarity level between the client and its neighbors, as well as the similarity to individual neighbors, mirroring the model's learning state. To determine the confidence \tilde{C}_i^t of client i , we first calculate the entropy using the following equation:

$$h_i^t = - \sum_{j \in C_i} e_{i,j}^t \log(e_{i,j}^t), \quad (10)$$

where h_i^t represents of node i 's uncertainty and $e_{i,j}^t \in (0, 1)$ represents the refined cosine similarity that comes from $e_{i,j}^t = \frac{\text{sim}(\phi_i, \phi_j) + 1}{2}$. Normalize $H^t = (h_1^t, \dots, h_m^t)$ to obtain \tilde{H}^t as follows:

$$\tilde{H}^t = \sigma(H^t), \quad (11)$$

where $\sigma(X) = \frac{1}{1+e^{-X}}$ is the sigmoid function. $\tilde{H}_i^t \in (0, 1)$ represents the i -th element of \tilde{H}^t .

A higher value of \tilde{H}_i suggests that client i is more challenging to distinguish, the neighbors with diverse distribution are lower. The confidence \tilde{C}_i^t of client i is then obtained by:

$$\tilde{C}_i^t = 1 - \tilde{H}_i^t. \quad (12)$$

With the confidence of the client given, we can now set the threshold θ_i for client i as:

$$\theta_i^t = \tau \tilde{C}_i^t, \quad (13)$$

where τ represents the global threshold, a constant. By comparing this threshold with $p_{i,j}^t$, we can determine the termination condition for the proposed greedy selection process and enable a flexible number of participating clients.

Remark 3.3. *Since $\tilde{C}_i^t \in (0, 1)$, the threshold θ_i will not exceed τ . Higher \tilde{C}_i values indicate closer alignment of neighbor distributions with the client, resulting in a smaller threshold and a greater chance of neighbor participation, potentially increasing the number of participating neighbors.*

3.4 Contribution-Awareness Aggregation

While we successfully identify and select friendly neighbors for collaboration, variations in data distributions among sampled users lead to differing contributions to cooperation. To utilize the selected neighbors' information more effectively, we introduce an aggregation strategy based on the Boltzmann distribution, using the loss of sampled clients to quantify their contributions. This aggregation strategy evaluates the impact of a client's distribution on the model \mathbf{x} , as expressed in the following formulation:

$$\varpi_{i,j}^t = \frac{e^{-F_j(\mathbf{w}_i, \beta_j; \xi_j)/T}}{Z}, \quad (14)$$

where T is the temperature and $Z = \sum_{i \in C_i} e^{-F_j(\mathbf{w}_i, \beta_j; \xi_j)/T}$ is the partition function. In this paper, we simply use $T = 1$ to obtain satisfactory results.

To enhance performance by smoothing loss between clients, we propose a moving average of current and previous round losses:

$$\tilde{F}_j(\mathbf{w}_i^t, \beta_j^t; \xi_j) = (1 - \gamma)F_j(\mathbf{w}_i^{t,K}, \beta_j^{t,K}; \xi_j) + \gamma F_j(\mathbf{w}_i^t, \beta_j^t; \xi_j), \quad (15)$$

where γ is a constant. Correspondingly, the aggregation distribution should be:

$$\varpi_{i,j}^t = \frac{e^{-\tilde{F}_j(\mathbf{w}_i^t, \beta_j^t; \xi_j)/T}}{Z}. \quad (16)$$

Remark 3.4. *The Boltzmann distribution balances contributions from different neighbors probabilistically. Better-performing neighbors have a higher influence on the client model, but it also allows for contributions from less-performing devices.*

4 Convergence Analysis

To ease the theoretical analysis of our work, we use the following widely used assumptions:

Assumption 1 (Smoothness). *For each client $i = \{1, \dots, m\}$, the function F_i is continuously differentiable. There exist constants $L_{\mathbf{w}}, L_{\beta}, L_{\mathbf{w}\beta}, L_{\beta\mathbf{w}}$ such that for each client $i = \{1, \dots, m\}$: $\nabla_{\mathbf{w}} f_i(\mathbf{w}_i, \beta_i)$ is $L_{\mathbf{w}}$ -Lipschitz with respect to \mathbf{w} and $L_{\mathbf{w}\beta}$ -Lipschitz with respect to β_i ; $\nabla_{\beta} f_i(\mathbf{w}_i, \beta_i)$ is L_{β} -Lipschitz with respect to β_i and $L_{\beta\mathbf{w}}$ -Lipschitz with respect to \mathbf{w}_i .*

Assumption 2 (Bounded Variance). *The stochastic gradients $\nabla_{\mathbf{w}} \hat{f}_i(w, \beta_i; \xi)$, $\nabla_{\beta} \hat{f}_i(w, \beta_i; \xi)$ satisfy for all $i \in [m]$, $w \in \mathbb{R}^{d_0}$, $\beta_i \in \mathbb{R}^{d_i}$:*

$$\mathbb{E} \left[\left\| \nabla_{\mathbf{w}} \hat{f}_i(w, \beta_i; \xi) - \nabla_{\mathbf{w}} f_i(w, \beta_i) \right\|^2 \right] \leq A_1 \left\| \nabla_{\mathbf{w}} f_i(w, \beta_i) \right\|^2 + \sigma_w^2, \quad (17)$$

$$\mathbb{E} \left[\left\| \nabla_{\beta} \hat{f}_i(w, \beta_i; \xi) - \nabla_{\beta} f_i(w, \beta_i) \right\|^2 \right] \leq A_2 \left\| \nabla_{\beta} f_i(w, \beta_i) \right\|^2 + \sigma_{\beta}^2, \quad (18)$$

for all $i \in [m]$, where $A_1, A_2, \sigma_w, \sigma_{\beta}$ are all positive constants.

Assumption 3 (Bounded Dissimilarity). *There is a positive constant $\lambda > 0$ such that for all $w \in \mathbb{R}^{d_0}$ and $\beta_i \in \mathbb{R}^{d_i}, i \in [i]$, we have*

$$\frac{1}{m} \sum_{i=1}^m \left\| \nabla f_i(w, \beta_i) \right\|^2 \leq \lambda \left\| \frac{1}{m} \sum_{i=1}^m \nabla f_i(w, \beta_i) \right\|^2 + \sigma_G^2. \quad (19)$$

Table 1: **Performance improvement of AFIND+**. We compare the performance of different sampling methods in DFL on CIFAR-10 and CIFAR-100 with both Dirichlet and Pathological distributions. The α represents the Dirichlet parameter and c represents sampling classes of pathological partition. The data is divided into 100 clients, with 10 clients sampled in each round for baselines. Each experiment comprises 500 communication rounds, with the number of local epochs set to 5. We measure the average test accuracy of all clients in each communication round and report the best performance attained across all rounds. The results are then averaged over three seeds. We highlight the best results by using **bold font**.

Algorithm	CIFAR-10				CIFAR-100			
	Dirichlet		Pathological		Dirichlet		Pathological	
	$\alpha = 0.1$	$\alpha = 0.5$	$c = 2$	$c = 5$	$\alpha = 0.1$	$\alpha = 0.5$	$c = 5$	$c = 10$
Local	48.44±0.44	62.36±0.51	86.52±0.56	70.96±0.48	32.21±0.52	29.52±1.12	75.43±0.89	53.06±0.90
FedAvg	55.29±0.04	78.24±0.21	59.81±0.41	56.87±0.58	45.42±0.26	46.48±1.29	27.20±0.81	35.29±0.62
Gossip	59.47±0.09	80.74±0.11	85.31±0.30	73.46±0.36	56.74±0.46	55.77±0.69	79.54±0.50	64.23±0.73
PENS	62.66±0.19	83.12±0.12	88.03±0.31	75.83±0.34	57.91±0.53	57.89±1.88	82.65±0.84	67.03±1.21
FedeRiCo	66.31±0.07	84.50±0.10	88.26±0.32	76.82±0.14	57.83±0.79	57.65±1.03	82.79±1.45	68.22±1.26
AFIND+	71.89±0.06	88.82±0.16	91.13±0.27	80.36±0.32	62.11±1.82	61.02±1.29	84.87±0.81	71.07±1.02

The above three assumptions are commonly used in both non-convex optimization and FL literature, see e.g. [30, 31, 32, 33, 34, 35]. For Assumption 1, to simplify the notation, we are making L as a consistent upper bound for $L_{\mathbf{w}}$ and L_{β} . For Assumption 3, if all local loss functions are identical (homogeneous distribution), then we have $\sigma_G = 0$.

Given the above assumptions, we can establish the following convergence rate of AFIND+ (Algorithm 1) for general nonconvex objectives.

Theorem 4.1. *Under Assumptions 1 to 3, and let local learning rate $\eta_k = \eta$, for all $k \geq 0$, where η is small enough to satisfy $\eta L \lambda \left(\frac{A_1}{m} + A_2 + 1 \right) + \lambda \eta^2 L^2 (K - 1) K (A_1 + 1) - 1 \leq 0$. The convergence upper bound of Algorithm 1 AFIND+ satisfies:*

$$\frac{1}{t} \sum_{t=0}^{T-1} \mathbb{E} \left[\left\| \frac{1}{m} \sum_{i=1}^m \nabla f_i(w^t, \beta_i^t) \right\|^2 \right] \leq \frac{2F}{\eta T} + \Phi, \quad (20)$$

where

$$\Phi = \eta L \lambda \left\{ \left(\frac{A_1}{m} + A_2 + 1 \right) \sigma_G^2 + \frac{\sigma_w^2}{m} + \sigma_{\beta}^2 \right\} + \eta^2 L^2 \sigma_G^2 (K - 1)^2 (A_1 + 1) + \eta^2 L^2 \sigma_w^2 (K - 1)^2, \quad (21)$$

where $F = \mathbb{E} \left[\frac{1}{m} \sum_{i=1}^m f_i(w^0, \beta_i^0) - f^* \right]$ and $w^t := \frac{1}{m} \sum_{i=1}^m w_i^t$ is a sequence of so-called virtual iterates.

The variables, such as variance term $\sigma_{\mathbf{w}}, \sigma_{\beta}, \sigma_G$, and Lipschitz constant L , all control the convergence bound. Let $\eta = \mathcal{O} \left(\frac{1}{\sqrt{TKL}} \right)$, the convergence rate of AFIND+ is:

$$\frac{1}{t} \sum_{t=0}^{T-1} \mathbb{E} \left[\left\| \frac{1}{m} \sum_{i=1}^m \nabla f_i(w^t, \beta_i^t) \right\|^2 \right] \leq \mathcal{O} \left(\frac{1}{\sqrt{T}} + \frac{1}{T} \right). \quad (22)$$

Due to space limitations, further details and complete proof are deferred to Appendix A.

5 Experiments

In this section, we conduct experiments to validate the effectiveness of AFIND+. Detailed implementation and additional results are provided in Appendix due to space limitations.

5.1 Experimental Setup

Datasets and Data partition. We evaluate the performance of the proposed algorithm on three real datasets: FEMNIST [36], CIFAR-10, and CIFAR-100 [37]. We consider two different scenarios for simulating non-identical distribution (non-IID) of data across federated learning, following [38]. (1) **Dirichlet**

Table 2: **Ablation study for AFIND+**. (i) Identification: Greedy sampling using a fixed number of participation. (ii) Threshold: Enable a flexible number of participation by confidence level threshold. (iii) Aggregation: Contribution-based aggregation.

Algorithm	CIFAR-10		CIFAR-100	
	$\alpha = 0.1$	$c = 5$	$\alpha = 0.1$	$c = 10$
FedAvg-FT	59.47±0.09	73.46±0.36	32.21±0.52	64.23±0.73
+ <i>i</i>	65.57±0.12	76.96±0.53	57.25±0.99	68.10±1.47
+ <i>i</i> + <i>ii</i>	68.89±0.08	78.95±0.20	58.02±0.83	69.60±0.91
+ <i>i</i> + <i>ii</i> + <i>iii</i>	71.89±0.06	80.36±0.32	62.11±1.82	71.07±1.02

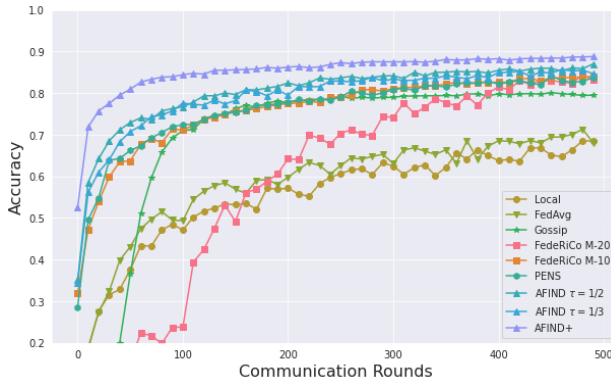


Figure 4: **Comparison of convergence performance of DFL using different collaboration strategies.** AFIND refers to our method AFIND+ with uniform aggregation.

Partition: we partition the training data according to a Dirichlet distribution $\text{Dir}(\alpha)$ for each client following the same distribution. We use $\alpha = 0.1$ and $\alpha = 0.5$ for all datasets. The smaller the α , the more heterogeneous the setting is. **(2) Pathological Partition:** we also evaluate with the pathological partition setup, as in [39], where each client is assigned a limited number of classes at random. We sample 2 and 5 classes for CIFAR-10, and 5 and 10 classes for CIFAR-100. The number of sampled classes is denoted as c in this paper.

Baselines and Models. We compare our methods with a diverse set of baselines, both from decentralized federated learning and personalized learning. A simple baseline called *Local* is implemented with each client separately, only conducting local training on their own data. Additionally, we include the centralized method FedAvg. For the sampling method of DFL, we list the existing and SOTA sampling methods, including the random method gossip sampling [24], the performance-based method PENS [19], and FederiCo [18]. In addition, we test the proposed method’s effectiveness in integrating with personalized FL algorithms, such as [40], Fed-FT [41], FOMO [39], and Dis-PFL [38]. All accuracy results are reported as the mean and standard deviation across three different random seeds. Unless specified otherwise, AFIND refers to AFIND+ without aggregation, with a global threshold $\tau = 0.5$ and momentum $\gamma = 0.9$. We use a CNN model for FEMNIST and CIFAR-10, and ResNet-18 for CIFAR-100. More training settings are detailed in Appendix C.3.

5.2 Performance Evaluation

AFIND+ achieves notable accuracy improvement over other sampling methods and local training methods in DFL. As shown in Table 1, AFIND+ outperforms other baselines with the best accuracy across different datasets and data heterogeneity scenarios. Specifically, on CIFAR-10, AFIND+ achieves 71.89% and 88.82% accuracy for Dirichlet $\alpha = 0.1$ and $\alpha = 0.5$, respectively, which is 5.32% and 4.32% higher than the best-competing method, FederiCo. Similarly, for Pathological datasets, AFIND+ achieves 91.13% and 80.36% accuracy, outperforming the state-of-the-art FederiCo by 2.87% and 3.54% for $c = 2$ and $c = 5$, respectively. On CIFAR-100, AFIND+ shows at least a 3.37% improvement for Dirichlet and a 2.08% improvement for Pathological over state-of-the-art results. We attribute this improvement to AFIND+’s ability to identify the right collaborators, assign aggregation weights based on their contributions,

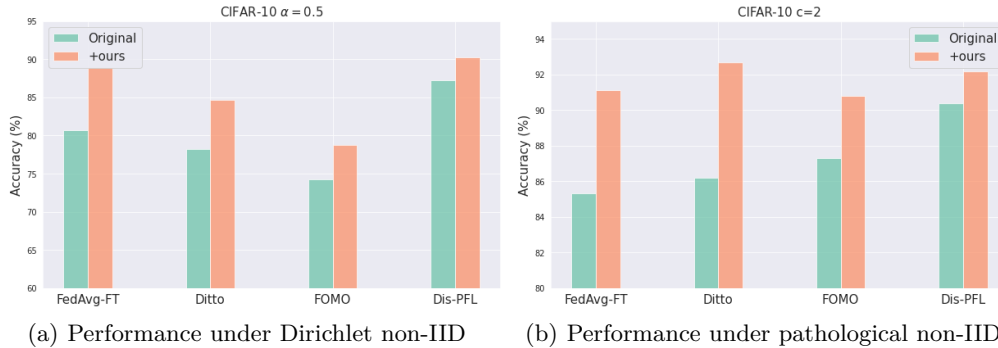


Figure 5: Improving the performance of Decentralized PFL methods compatible with AFIND+.

and adaptively adjust the search space to include appropriate collaborators while excluding inappropriate ones, as demonstrated in the ablation study for AFIND+.

AFIND+ converges faster than other sampling methods. Figure 4 demonstrates the superior convergence performance of our sampling method on FEMNIST. Additionally, we observe that a smaller global threshold τ leads to slightly better performance, but the performance remains robust to the hyperparameter τ . Moreover, when integrated with the importance-based aggregation method, AFIND+ shows much better performance than others, indicating greater efficiency in training. This implies that there are differences in contribution even among the correct collaborators being sampled, and our aggregation method has the ability to capture the contribution among collaborators.

AFIND+ compatibility with PFL algorithms enhances performance in DFL. Figure 5 illustrates that AFIND+ is compatible with various PFL algorithms when applied in DFL. Despite variations, the improvement remains significant, resulting in an approximately 3% increase in performance.

All the components of AFIND+ are necessary and beneficial. We conduct the ablation study for AFIND+ in Table 2. It demonstrates that the identification of the right neighbors for collaboration, the adaptive threshold for client participation, and the contribution-aware aggregation method all contribute to improving the performance of DFL. FedAvg-FT refers to the personalized DFL algorithm with random sampling as the baseline, and our sampling method, aided by the threshold, significantly improves accuracy on the Dirichlet distribution by approximately 10% for CIFAR-10 and 20% for CIFAR-100. Additionally, the proposed aggregation method further enhances performance by approximately 2% for both CIFAR-10 and CIFAR-100.

Additional experiments demonstrate AFIND+’s superiority, including: (1) an ablation study for the threshold parameter τ ; (2) an ablation study for network topologies; and (3) a privacy evaluation, provided in Appendix C.4.

6 Conclusions, Limitations and Future Works

In this paper, we introduce AFIND+, a novel DFL client collaboration optimization algorithm that identifies the right collaborators, allows flexible participation, and uses contribution-based aggregation. We empirically demonstrate its superiority over other DFL sampling algorithms and offer a convergence guarantee. However, ensuring its effectiveness in dynamic networks remains a challenge due to the varying availability of neighbors, which affects the search space of the sampling distribution. We leave this as a future research direction.

References

- [1] Brendan McMahan, Eider Moore, Daniel Ramage, Seth Hampson, and Blaise Aguera y Arcas. Communication-efficient learning of deep networks from decentralized data. In *Artificial intelligence and statistics*, pages 1273–1282. PMLR, 2017.
- [2] Georgios A Kaissis, Marcus R Makowski, Daniel Rückert, and Rickmer F Braren. Secure, privacy-preserving and federated machine learning in medical imaging. *Nature Machine Intelligence*, 2(6):305–311, 2020.
- [3] Yuris Mulya Saputra, Dinh Thai Hoang, Diep N Nguyen, Eryk Dutkiewicz, Markus Dominik Mueck, and Srikathyayani Srikanteswara. Energy demand prediction with federated learning for electric vehicle networks. In *2019 IEEE global communications conference (GLOBECOM)*, pages 1–6. IEEE, 2019.
- [4] Youyang Qu, Shiva Raj Pokhrel, Sahil Garg, Longxiang Gao, and Yong Xiang. A blockchained federated learning framework for cognitive computing in industry 4.0 networks. *IEEE Transactions on Industrial Informatics*, 17(4):2964–2973, 2020.
- [5] Yae Jee Cho, Jianyu Wang, and Gauri Joshi. Client selection in federated learning: Convergence analysis and power-of-choice selection strategies. *arXiv preprint arXiv:2010.01243*, 2020.
- [6] Lin Wang, YongXin Guo, Tao Lin, and Xiaoying Tang. Delta: Diverse client sampling for fasting federated learning. *arXiv preprint arXiv:2205.13925*, 2022.
- [7] Guangyuan Shen, Dehong Gao, DuanXiao Song, Xukai Zhou, Shirui Pan, Wei Lou, Fang Zhou, et al. Fast heterogeneous federated learning with hybrid client selection. *arXiv preprint arXiv:2208.05135*, 2022.
- [8] Jianyu Wang, Zachary Charles, Zheng Xu, Gauri Joshi, H Brendan McMahan, Maruan Al-Shedivat, Galen Andrew, Salman Avestimehr, Katharine Daly, Deepesh Data, et al. A field guide to federated optimization. *arXiv preprint arXiv:2107.06917*, 2021.
- [9] Matias Mendieta, Taojiannan Yang, Pu Wang, Minwoo Lee, Zhengming Ding, and Chen Chen. Local learning matters: Rethinking data heterogeneity in federated learning. In *Proceedings of the IEEE/CVF Conference on Computer Vision and Pattern Recognition*, pages 8397–8406, 2022.
- [10] Anusha Lalitha, Osman Cihan Kilinc, Tara Javidi, and Farinaz Koushanfar. Peer-to-peer federated learning on graphs. *arXiv preprint arXiv:1901.11173*, 2019.
- [11] Abdurakhmon Sadiev, Ekaterina Borodich, Aleksandr Beznosikov, Darina Dvinskikh, Saveliy Chezhegov, Rachael Tappenden, Martin Takáč, and Alexander Gasnikov. Decentralized personalized federated learning: Lower bounds and optimal algorithm for all personalization modes. *EURO Journal on Computational Optimization*, 10:100041, 2022.
- [12] Eunjeong Jeong and Marios Kountouris. Personalized decentralized federated learning with knowledge distillation. *arXiv preprint arXiv:2302.12156*, 2023.
- [13] Peter Kairouz, H Brendan McMahan, Brendan Avent, Aurélien Bellet, Mehdi Bennis, Arjun Nitin Bhagoji, Kallista Bonawitz, Zachary Charles, Graham Cormode, Rachel Cummings, et al. Advances and open problems in federated learning. *arXiv preprint arXiv:1912.04977*, 2019.
- [14] Ang Li, Jingwei Sun, Xiao Zeng, Mi Zhang, Hai Li, and Yiran Chen. Fedmask: Joint computation and communication-efficient personalized federated learning via heterogeneous masking. In *Proceedings of the 19th ACM Conference on Embedded Networked Sensor Systems*, pages 42–55, 2021.
- [15] Abhijit Guha Roy, Shayan Siddiqui, Sebastian Pölsterl, Nassir Navab, and Christian Wachinger. Braintorrent: A peer-to-peer environment for decentralized federated learning. *arXiv preprint arXiv:1905.06731*, 2019.
- [16] Enrique Tomás Martínez Beltrán, Mario Quiles Pérez, Pedro Miguel Sánchez Sánchez, Sergio López Bernal, Gérôme Bovet, Manuel Gil Pérez, Gregorio Martínez Pérez, and Alberto Huertas Celdrán. Decentralized federated learning: Fundamentals, state of the art, frameworks, trends, and challenges. *IEEE Communications Surveys & Tutorials*, 2023.
- [17] Yuben Qu, Haipeng Dai, Yan Zhuang, Jiafa Chen, Chao Dong, Fan Wu, and Song Guo. Decentralized federated learning for uav networks: Architecture, challenges, and opportunities. *IEEE Network*, 35(6):156–162, 2021.
- [18] Yi Sui, Junfeng Wen, Yenson Lau, Brendan Leigh Ross, and Jesse C Cresswell. Find your friends: Personalized federated learning with the right collaborators. *arXiv preprint arXiv:2210.06597*, 2022.

- [19] Noa Onoszko, Gustav Karlsson, Olof Mogren, and Edvin Listo Zec. Decentralized federated learning of deep neural networks on non-iid data. *arXiv preprint arXiv:2107.08517*, 2021.
- [20] Yann Fraboni, Richard Vidal, Laetitia Kameni, and Marco Lorenzi. On the impact of client sampling on federated learning convergence. *arXiv preprint arXiv:2107.12211*, 2021.
- [21] Rui Liu, Pengwei Xing, Zichao Deng, Anran Li, Cuntai Guan, and Han Yu. Federated graph neural networks: Overview, techniques and challenges. *arXiv preprint arXiv:2202.07256*, 2022.
- [22] Jiawen Kang, Dongdong Ye, Jiangtian Nie, Jiang Xiao, Xianjun Deng, Siming Wang, Zehui Xiong, Rong Yu, and Dusit Niyato. Blockchain-based federated learning for industrial metaverses: Incentive scheme with optimal aoi. In *2022 IEEE International Conference on Blockchain (Blockchain)*, pages 71–78. IEEE, 2022.
- [23] Bo Li, Mikkel N Schmidt, Tommy S Alstrøm, and Sebastian U Stich. On the effectiveness of partial variance reduction in federated learning with heterogeneous data. *arXiv preprint arXiv:2212.02191*, 2022.
- [24] István Hegedűs, Gábor Danner, and Márk Jelasity. Gossip learning as a decentralized alternative to federated learning. In *Distributed Applications and Interoperable Systems: 19th IFIP WG 6.1 International Conference, DAIS 2019*, pages 74–90. Springer, 2019.
- [25] Tao Sun, Dongsheng Li, and Bao Wang. Decentralized federated averaging. *IEEE Transactions on Pattern Analysis and Machine Intelligence*, 45(4):4289–4301, 2022.
- [26] Ravikumar Balakrishnan, Tian Li, Tianyi Zhou, Nageen Himayat, Virginia Smith, and Jeff Bilmes. Diverse client selection for federated learning: Submodularity and convergence analysis. In *ICML 2021 International Workshop on Federated Learning for User Privacy and Data Confidentiality*, Virtual, July 2021.
- [27] Ozan Sener and Silvio Savarese. Active learning for convolutional neural networks: A core-set approach. *arXiv preprint arXiv:1708.00489*, 2017.
- [28] Baharan Mirzasoleiman, Jeff Bilmes, and Jure Leskovec. Coresets for data-efficient training of machine learning models. In *International Conference on Machine Learning*, pages 6950–6960. PMLR, 2020.
- [29] Linjie Zheng, Yonghua Jiang, Hongkui Jiang, Chao Tang, Weidong Jiao, Zhuoqi Shi, and Attiq Ur Rehman. Adaptive dynamic threshold graph neural network: A novel deep learning framework for cross-condition bearing fault diagnosis. *Machines*, 12(1):18, 2023.
- [30] Hao Sun, Li Shen, Qihuang Zhong, Liang Ding, Shixiang Chen, Jingwei Sun, Jing Li, Guangzhong Sun, and Dacheng Tao. Adasam: Boosting sharpness-aware minimization with adaptive learning rate and momentum for training deep neural networks. *Neural Networks*, 169:506–519, 2024.
- [31] Haibo Yang, Minghong Fang, and Jia Liu. Achieving linear speedup with partial worker participation in non-iid federated learning. *arXiv preprint arXiv:2101.11203*, 2021.
- [32] Anastasia Koloskova, Nicolas Loizou, Sadra Boreiri, Martin Jaggi, and Sebastian Stich. A unified theory of decentralized sgd with changing topology and local updates. In *International Conference on Machine Learning*, pages 5381–5393. PMLR, 2020.
- [33] Tao Lin, Sai Praneeth Karimireddy, Sebastian U Stich, and Martin Jaggi. Quasi-global momentum: Accelerating decentralized deep learning on heterogeneous data. *arXiv preprint arXiv:2102.04761*, 2021.
- [34] Farzin Haddadpour and Mehrdad Mahdavi. On the convergence of local descent methods in federated learning. *arXiv preprint arXiv:1910.14425*, 2019.
- [35] Filip Hanzely, Boxin Zhao, and Mladen Kolar. Personalized federated learning: A unified framework and universal optimization techniques. *arXiv preprint arXiv:2102.09743*, 2021.
- [36] Sebastian Caldas, Sai Meher Karthik Duddu, Peter Wu, Tian Li, Jakub Konečný, H Brendan McMahan, Virginia Smith, and Ameet Talwalkar. Leaf: A benchmark for federated settings. *arXiv preprint arXiv:1812.01097*, 2018.
- [37] Alex Krizhevsky, Geoffrey Hinton, et al. Learning multiple layers of features from tiny images. *Toronto, ON, Canada*, 2009.
- [38] Rong Dai, Li Shen, Fengxiang He, Xinmei Tian, and Dacheng Tao. Dispfl: Towards communication-efficient personalized federated learning via decentralized sparse training. *arXiv preprint arXiv:2206.00187*, 2022.
- [39] Michael Zhang, Karan Sapra, Sanja Fidler, Serena Yeung, and Jose M Alvarez. Personalized federated learning with first order model optimization. *arXiv preprint arXiv:2012.08565*, 2020.

- [40] Tian Li, Shengyuan Hu, Ahmad Beirami, and Virginia Smith. Ditto: Fair and robust federated learning through personalization. In *International Conference on Machine Learning*, pages 6357–6368. PMLR, 2021.
- [41] Gary Cheng, Karan Chadha, and John Duchi. Fine-tuning is fine in federated learning. *arXiv preprint arXiv:2108.07313*, 3, 2021.
- [42] Leon Witt, Mathis Heyer, Kentaroh Toyoda, Wojciech Samek, and Dan Li. Decentral and incentivized federated learning frameworks: A systematic literature review. *IEEE Internet of Things Journal*, 2022.
- [43] Edoardo Gabrielli, Giovanni Pica, and Gabriele Tolomei. A survey on decentralized federated learning. *arXiv preprint arXiv:2308.04604*, 2023.
- [44] Lingling Wang, Xueqin Zhao, Zhongkai Lu, Lin Wang, and Shouxun Zhang. Enhancing privacy preservation and trustworthiness for decentralized federated learning. *Information Sciences*, 628:449–468, 2023.
- [45] Shuzhen Chen, Dongxiao Yu, Yifei Zou, Jiguo Yu, and Xiuzhen Cheng. Decentralized wireless federated learning with differential privacy. *IEEE Transactions on Industrial Informatics*, 18(9):6273–6282, 2022.
- [46] Alysa Ziyang Tan, Han Yu, Lizhen Cui, and Qiang Yang. Towards personalized federated learning. *IEEE Transactions on Neural Networks and Learning Systems*, 2022.
- [47] H. Brendan McMahan, Eider Moore, Daniel Ramage, and Blaise Agüera y Arcas. Federated learning of deep networks using model averaging. *CoRR*, abs/1602.05629, 2016.
- [48] Viraj Kulkarni, Milind Kulkarni, and Aniruddha Pant. Survey of personalization techniques for federated learning. In *2020 Fourth World Conference on Smart Trends in Systems, Security and Sustainability (WorldS4)*, pages 794–797. IEEE, 2020.
- [49] Guangsheng Yu, Xu Wang, Caijun Sun, Qin Wang, Ping Yu, Wei Ni, and Ren Ping Liu. Ironforge: An open, secure, fair, decentralized federated learning. *IEEE Transactions on Neural Networks and Learning Systems*, 2023.
- [50] Bin Wang, Jun Fang, Hongbin Li, Xiaojun Yuan, and Qing Ling. Confederated learning: Federated learning with decentralized edge servers. *IEEE Transactions on Signal Processing*, 71:248–263, 2023.
- [51] Xiaokang Zhou, Wei Liang, I Kevin, Kai Wang, Zheng Yan, Laurence T Yang, Wei Wei, Jianhua Ma, and Qun Jin. Decentralized p2p federated learning for privacy-preserving and resilient mobile robotic systems. *IEEE Wireless Communications*, 30(2):82–89, 2023.
- [52] Huiqiang Chen, Tianqing Zhu, Tao Zhang, Wanlei Zhou, and Philip S Yu. Privacy and fairness in federated learning: on the perspective of trade-off. *ACM Computing Surveys*, 2023.
- [53] Zheng-yi Chai, Chuan-dong Yang, and Ya-lun Li. Communication efficiency optimization in federated learning based on multi-objective evolutionary algorithm. *Evolutionary Intelligence*, 16(3):1033–1044, 2023.
- [54] Omair Rashed Abdulwareth Almanifi, Chee-Onn Chow, Mau-Luen Tham, Joon Huang Chuah, and Jeevan Kanesan. Communication and computation efficiency in federated learning: A survey. *Internet of Things*, 22:100742, 2023.
- [55] Giovanni Paragliola and Antonio Coronato. Definition of a novel federated learning approach to reduce communication costs. *Expert Systems with Applications*, 189:116109, 2022.
- [56] Yurii Nesterov et al. *Lectures on convex optimization*, volume 137. Springer, 2018.
- [57] Martin Abadi, Andy Chu, Ian Goodfellow, H Brendan McMahan, Ilya Mironov, Kunal Talwar, and Li Zhang. Deep learning with differential privacy. In *Proceedings of the 2016 ACM SIGSAC conference on computer and communications security*, pages 308–318, 2016.

Contents of Appendix

1	Introduction	1
2	Related Works	3
3	AFIND+: Adaptive Collaboration for DFL	3
3.1	Preliminary	3
3.2	Identify Right Neighbors	4
3.3	Adaptive Threshold for Flexible Neighbor Participation	5
3.4	Contribution-Awareness Aggregation	7
4	Convergence Analysis	7
5	Experiments	8
5.1	Experimental Setup	8
5.2	Performance Evaluation	9
6	Conclusions, Limitations and Future Works	10
A	An extension of Related Works	14
B	Theoretical Analysis and Proof	15
B.1	Useful Lemmas	15
B.2	Proof of Theorem 3.5	21
C	Additional Experiment Results and Experiment Details	24
C.1	Toy examples	24
C.2	Experimental Environment	25
C.3	Experiment setup	25
C.4	Additional Experimental Results	26

A An extension of Related Works

Decentralized Federated Learning (DFL) aligns local models through peer-to-peer communication, with clients connecting solely to their neighbors [21, 22, 23]. This structure minimizes single-point failure risks compared to Centralized Federated Learning (CFL), yet privacy and security concerns persist [42, 43]. Extensive research addresses these challenges in DFL, focusing on privacy and diverse data distribution [44, 45]. Foundational work by [46] and [47] advances decentralized collaboration, emphasizing data privacy preservation in collaborative learning. Recent studies highlight the effectiveness of personalized models in DFL, given each client’s local model [48, 49, 50]. Despite these advancements, client sampling complexity in the DFL framework remains a prominent research area.

Client Selection in DFL is a continuing challenge, with limited research focused on client sampling in Decentralized Federated Learning. [24] employs gossip sampling, which randomly selects clients. [19] suggests a heuristic, performance-based sampling method, where clients share model parameters with others to evaluate loss values; a lower loss value indicates a more preferable client for sampling. [18] utilizes expectation maximization in a personalized DFL algorithm, selecting neighbors based on the exponent of negative loss. While these studies agree that selecting neighbors with similar data distributions enhances DFL performance, our approach is distinct. We propose using client features as proxies for distribution similarity. Moreover, unlike these studies which focus on fixed-number sampling, we introduce an adaptive threshold for neighbor selection, allowing for a variable number of participating neighbors.

DFL others. In addition to client sampling algorithms, FL faces other challenges such as privacy preservation [44, 51, 52] and communication efficiency [53, 54, 55]. We show that AFIND+ is compatible with existing privacy and communication enhancement methods, as shown in Section 5.

B Theoretical Analysis and Proof

In this section, we provide the analysis of Theorem 3.5, i.e., the convergence analysis.

B.1 Useful Lemmas

In this subsection, we will present some useful lemmas before giving the complete convergence proof.

We start by introducing additional notation, following from [35]. We set $t_p = p \cdot K$, where $K \in \mathbb{N}^+$ is the length of the averaging period. Let $t_p = pK + K - 1 = t_{p+1} - 1 = v_p$. Denote the total number of iterations as T and assume that $T = k_{\bar{p}}$ for some $\bar{p} \in \mathbb{N}^+$. The final result is set to be that $\hat{w} = w^T$ and $\hat{\beta}_m = \beta_i^T$ for all $i \in [m]$. We assume that the solution to (2) is $w^*, \beta_1^*, \dots, \beta_m^*$ and that the optimal value is f^* . Let $w^t = \frac{1}{m} \sum_{i=1}^m w_i^t$ for all t . Note that this quantity will not be actually computed in practice unless $t = t_p$ for some $p \in \mathbb{N}$, where we have $w^{t_p} = w_i^{t_p}$ for all $i \in [m]$. In addition, let $\xi_i^t = \{\xi_{1,i}^t, \xi_{2,i}^t, \dots, \xi_{B,i}^t\}$ and $\xi^t = \{\xi_1^t, \xi_2^t, \dots, \xi_m^t\}$. Let

$$g_i^t = \frac{1}{B} \nabla F_i(w_i^t, \beta_i^t; \xi_i^t), \quad (23)$$

where $\nabla F_i(w_i^t, \beta_i^t; \xi_i^t) = \sum_{j=1}^B \nabla F_i(w_i^t, \beta_i^t; \xi_{j,i}^t)$.

When the gradient is unbiased, we get

$$\mathbb{E}[g_i^t] = \nabla F_i(w_i^t, \beta_i^t). \quad (24)$$

Let $g_{i,1}^t = \frac{1}{B} \nabla_w F_i(w_i^t, \beta_i^t; \xi_i^t)$, $g_{i,2}^t = \frac{1}{B} \nabla_{\beta_i} F_i(w_i^t, \beta_i^t; \xi_i^t)$, so that $g_i^t = \left((g_{i,1}^t)^\top, (g_{i,2}^t)^\top \right)^\top$.

Thus, the parameter is updated by :

$$(w_i^{t+1}, \beta_i^{t+1}) = (w_i^t, \beta_i^t) - \eta_t g_i^t. \quad (25)$$

Then we define

$$h^t = \frac{1}{m} \sum_{i=1}^m g_{i,1}^t, \quad V^t = \frac{1}{m} \sum_{i=1}^m \|w_i^t - w^t\|^2. \quad (26)$$

Then $w^{t+1} = w^t - \eta_t h^t$ for all t .

We denote the Bregman divergence associated with F_i for x_i and \bar{x}_i as

$$D_{F_i}(x_i, \bar{x}_i) := f_i(x_i) - f_i(\bar{x}_i) - \langle \nabla f_i(\bar{x}_i), x_i - \bar{x}_i \rangle. \quad (27)$$

Finally, we define the sum of residuals as

$$r^t = \|w^t - w^*\|^2 + \frac{1}{m} \sum_{i=1}^m \|\beta_i^t - \beta_i^*\|^2 = \frac{1}{m} \sum_{i=1}^m \|\hat{x}_i^t - x_i^*\|^2 \quad (28)$$

and let $\sigma_G^2 = \frac{1}{m} \sum_{i=1}^m \|\nabla f_i(x_i^*)\|^2$.

Following the standard results in [56], we present the following proposition:

Proposition B.1. *If the function f is differentiable and L -smooth, then*

$$f(x) - f(y) - \langle \nabla f(y), x - y \rangle \leq \frac{L}{2} \|x - y\|^2. \quad (29)$$

If f is also convex, then

$$\|\nabla f(x) - \nabla f(y)\|^2 \leq 2LD_f(x, y) \forall x, y. \quad (30)$$

For all vectors x, y , we have

$$2\langle x, y \rangle \leq \xi \|x\|^2 + \xi^{-1} \|y\|^2, \quad \forall \xi > 0, \quad (31)$$

$$-\langle x, y \rangle = -\frac{1}{2} \|x\|^2 - \frac{1}{2} \|y\|^2 + \frac{1}{2} \|x - y\|^2. \quad (32)$$

For vectors v_1, v_2, \dots, v_n , by Jensen's inequality and the convexity of the map: $x \mapsto \|x\|^2$, we have

$$\left\| \frac{1}{n} \sum_{i=1}^n v_i \right\|^2 \leq \frac{1}{n} \sum_{i=1}^n \|v_i\|^2 \quad (33)$$

Then, we provide some useful lemmas:

Lemma B.2. *Suppose Assumption 1 holds. Given $\{x_i^t\}_{i \in [m]}$, we have:*

$$\mathbb{E} \left[\frac{1}{m} \sum_{i=1}^m F_i(\hat{x}_m^{k+1}) \right] - \frac{1}{m} \sum_{i=1}^m F_i(\hat{x}_i^t) \quad (34)$$

$$\leq -\eta \left\langle \frac{1}{m} \sum_{i=1}^m \nabla_w F_i(\hat{x}_i^t), \frac{1}{m} \sum_{i=1}^m \nabla_w F_i(x_i^t) \right\rangle \quad (35)$$

$$- \frac{\eta}{m} \sum_{i=1}^m \langle \nabla_{\beta_i} F_i(\hat{x}_i^t), \nabla_{\beta_i} F_i(x_i^t) \rangle \quad (36)$$

$$+ \frac{\eta^2 L}{2} \mathbb{E} [\|h^t\|^2] + \frac{\eta^2 L}{2m} \sum_{i=1}^m \mathbb{E} [\|g_{i,2}^t\|^2], \quad (37)$$

where the expectation is taken with respect to the randomness in ξ^t .

Proof. By the L -smoothness assumption on $F_i(\cdot)$ and (29), we have

$$\begin{aligned} F_i(\hat{x}_m^{k+1}) - F_i(\hat{x}_i^t) - \langle \nabla F_i(\hat{x}_i^t), \hat{x}_m^{k+1} - \hat{x}_i^t \rangle \\ \leq \frac{L}{2} \|\hat{x}_m^{k+1} - \hat{x}_i^t\|^2. \end{aligned} \quad (38)$$

Thus, we have

$$\begin{aligned} F_i(\hat{x}_m^{k+1}) - F_i(\hat{x}_i^t) &\leq -\eta \langle \nabla_w F_i(\hat{x}_i^t), h^t \rangle \\ &\quad - \eta \langle \nabla_{\beta_i} F_i(\hat{x}_i^t), g_{i,2}^t \rangle + \frac{\eta^2 L}{2} \|h^t\|^2 + \frac{\eta^2 L}{2} \|g_{i,2}^t\|^2, \end{aligned} \quad (39)$$

which implies that

$$\begin{aligned} \frac{1}{m} \sum_{i=1}^m F_i(\hat{x}_m^{k+1}) - \frac{1}{m} \sum_{i=1}^m F_i(\hat{x}_i^t) &\leq \\ -\eta \left\langle \frac{1}{m} \sum_{i=1}^m \nabla_w F_i(\hat{x}_i^t), h^t \right\rangle - \frac{\eta}{m} \sum_{i=1}^m \langle \nabla_{\beta_i} F_i(\hat{x}_i^t), g_{i,2}^t \rangle \\ + \frac{\eta^2 L}{2} \|h^t\|^2 + \frac{\eta^2 L}{2m} \sum_{i=1}^m \|g_{i,2}^t\|^2. \end{aligned} \quad (40)$$

The result follows by taking the expectation with respect to the randomness in ξ^t , while keeping the other quantities fixed. \square

Lemma B.3. *Suppose Assumptions 2 and 3 hold. Given $\{x_i^t\}_{i \in [m]}$, we have*

$$\mathbb{E} \left[\|h^t\|^2 \right] + \frac{1}{m} \sum_{i=1}^m \mathbb{E} \left[\|g_{i,2}^t\|^2 \right] \quad (41)$$

$$\leq \left(\frac{A_1}{m} + A_2 + 1 \right) \frac{1}{m} \sum_{i=1}^m \|F_i(x_i^t)\|^2 + \frac{\sigma_w^2}{m} + \sigma_\beta^2 \quad (42)$$

$$\leq \lambda \left(\frac{A_1}{m} + A_2 + 1 \right) \left\| \frac{1}{m} \sum_{i=1}^m \nabla F_i(x_i^t) \right\|^2 + \left(\frac{A_1}{m} + A_2 + 1 \right) \sigma_G^2 + \frac{\sigma_w^2}{m} + \sigma_\beta^2, \quad (43)$$

where the expectation is taken only with respect to the randomness in ξ^t .

Proof. Note that

$$\mathbb{E} \left[\|h^t\|^2 \right] = \mathbb{E} \left[\left\| \frac{1}{m} \sum_{i=1}^m g_{i,1}^t \right\|^2 \right] \quad (44)$$

$$\stackrel{(a)}{=} \mathbb{E} \left[\left\| \frac{1}{m} \sum_{i=1}^m (g_{i,1}^t - \nabla_w F_i(x_i^t)) \right\|^2 \right] + \left\| \frac{1}{m} \sum_{i=1}^m \nabla_w F_i(x_i^t) \right\|^2 \quad (45)$$

$$\stackrel{(b)}{=} \frac{1}{m^2} \sum_{i=1}^m \mathbb{E} \left[\|g_{i,1}^t - \nabla_w F_i(x_i^t)\|^2 \right] + \left\| \frac{1}{m} \sum_{i=1}^m \nabla_w F_i(x_i^t) \right\|^2 \quad (46)$$

$$\stackrel{(c)}{\leq} \frac{1}{m^2} \sum_{i=1}^m \left(A_1 \|\nabla F_i(x_i^t)\|^2 + \sigma_w^2 \right) + \left\| \frac{1}{m} \sum_{i=1}^m \nabla_w F_i(x_i^t) \right\|^2 \quad (47)$$

$$\stackrel{(d)}{\leq} \frac{A_1}{m^2} \sum_{i=1}^m \|\nabla F_i(x_i^t)\|^2 + \frac{\sigma_w^2}{m} + \frac{1}{m} \sum_{i=1}^m \|\nabla_w f_i(x_i^t)\|^2, \quad (48)$$

where (a) is attributed to the unbiased nature of $g_{i,1}^t$, (b) is a consequence of the independence of $\xi_1^k, \xi_2^k, \dots, \xi_i^k$, (c) is based on Assumption 2, and (d) follows from (33).

We also have

$$\begin{aligned} \frac{1}{m} \sum_{i=1}^m \mathbb{E} [\|g_{i,2}^t\|^2] &= \frac{1}{m} \sum_{i=1}^m \mathbb{E} [\|g_{i,2}^t - \nabla_{\beta_i} F_i(x_i^t)\|^2] \\ &+ \frac{1}{m} \sum_{i=1}^m \|\nabla_{\beta_i} F_i(x_i^t)\|^2 \end{aligned} \quad (49)$$

$$\leq \frac{A_2}{m} \sum_{i=1}^m \left\| \nabla F_i(x_i^t) \right\|^2 + \sigma_\beta^2 + \frac{1}{m} \sum_{i=1}^m \left\| \nabla_{\beta_i} F_i(x_i^t) \right\|^2. \quad (50)$$

□

Lemma B.4. *Under Assumption 1, we have*

$$\begin{aligned} & - \eta \left\langle \frac{1}{m} \sum_{i=1}^m \nabla_w F_i(\hat{x}_i^t), \frac{1}{m} \sum_{i=1}^m \nabla_w F_i(x_i^t) \right\rangle \\ & - \frac{\eta}{m} \sum_{i=1}^m \langle \nabla_{\beta_i} F_i(\hat{x}^k), \nabla_{\beta_i} F_i(x_i^t) \rangle \end{aligned} \quad (51)$$

$$\begin{aligned} & \leq -\frac{\eta}{2} \left\| \frac{1}{m} \sum_{i=1}^m \nabla F_i(\hat{x}_i^t) \right\|^2 - \frac{\eta}{2} \left\| \frac{1}{m} \sum_{i=1}^m \nabla F_i(x_i^t) \right\|^2 \\ & + \frac{\eta L^2}{2} V^t \end{aligned} \quad (52)$$

Proof. By (32), we have

$$- \eta \left\langle \frac{1}{m} \sum_{i=1}^m \nabla_w F_i(\hat{x}_i^t), \frac{1}{m} \sum_{i=1}^m \nabla_w F_i(x_i^t) \right\rangle \quad (53)$$

$$\begin{aligned} & = -\frac{\eta}{2} \left\| \frac{1}{m} \sum_{i=1}^m \nabla_w F_i(\hat{x}_i^t) \right\|^2 - \frac{\eta}{2} \left\| \frac{1}{m} \sum_{i=1}^m \nabla_w F_i(x_i^t) \right\|^2 \\ & + \frac{\eta}{2} \left\| \frac{1}{m} \sum_{i=1}^m (\nabla_w F_i(\hat{x}_i^t) - \nabla_w F_i(x_i^t)) \right\|^2 \end{aligned} \quad (54)$$

$$\begin{aligned} & \leq -\frac{\eta}{2} \left\| \frac{1}{m} \sum_{i=1}^m \nabla_w F_i(\hat{x}_i^t) \right\|^2 - \frac{\eta}{2} \left\| \frac{1}{m} \sum_{i=1}^m \nabla_w F_i(x_i^t) \right\|^2 \\ & + \frac{\eta}{2m} \sum_{i=1}^m \|\nabla_w F_i(\hat{x}_i^t) - \nabla_w F_i(x_i^t)\|^2, \end{aligned} \quad (55)$$

where the last inequality follows from (33). In addition,

$$\begin{aligned} & - \eta \langle \nabla_{\beta_i} F_i(\hat{x}^k), \nabla_{\beta_i} F_i(x_i^t) \rangle = -\frac{\eta}{2} \|\nabla_{\beta_i} F_i(\hat{x}_i^t)\|^2 \\ & - \frac{\eta}{2} \|\nabla_{\beta_i} F_i(x_i^t)\|^2 + \frac{\eta}{2} \|\nabla_{\beta_i} F_i(\hat{x}_i^t) - \nabla_{\beta_i} F_i(x_i^t)\|^2. \end{aligned} \quad (56)$$

Therefore, we have

$$\begin{aligned}
& -\frac{\eta}{m} \langle \nabla_{\beta_i} F_i(\hat{x}^k), \nabla_{\beta_i} F_i(x_i^t) \rangle \\
&= -\frac{\eta}{2m} \sum_{i=1}^m \|\nabla_{\beta_i} F_i(\hat{x}_i^t)\|^2 - \frac{\eta}{2m} \sum_{i=1}^m \|\nabla_{\beta_i} F_i(x_i^t)\|^2 \\
& \quad + \frac{\eta}{2m} \sum_{i=1}^m \|\nabla_{\beta_i} F_i(\hat{x}_i^t) - \nabla_{\beta_i} F_i(x_i^t)\|^2
\end{aligned} \tag{57}$$

$$\begin{aligned}
& \leq -\frac{\eta}{2} \left\| \frac{1}{m} \sum_{i=1}^m \nabla_{\beta_i} F_i(\hat{x}_i^t) \right\|^2 - \frac{\eta}{2} \left\| \frac{1}{m} \sum_{i=1}^m \nabla_{\beta_i} F_i(x_i^t) \right\|^2 \\
& \quad + \frac{\eta}{2m} \sum_{i=1}^m \|\nabla_{\beta_i} F_i(\hat{x}_i^t) - \nabla_{\beta_i} F_i(x_i^t)\|^2.
\end{aligned} \tag{58}$$

Combining the above equations, we have

$$\begin{aligned}
& -\eta \left\langle \frac{1}{m} \sum_{i=1}^m \nabla_w F_i(\hat{x}_i^t), \frac{1}{m} \sum_{i=1}^m \nabla_w F_i(x_i^t) \right\rangle \\
& -\frac{\eta}{m} \sum_{i=1}^m \langle \nabla_{\beta_i} F_i(\hat{x}_i^t), \nabla_{\beta_i} F_i(x_i^t) \rangle
\end{aligned} \tag{59}$$

$$\begin{aligned}
& \leq -\frac{\eta}{2} \left\| \frac{1}{m} \sum_{i=1}^m \nabla F_i(\hat{x}_i^t) \right\|^2 - \frac{\eta}{2} \left\| \frac{1}{m} \sum_{i=1}^m \nabla F_i(x_i^t) \right\|^2 \\
& \quad + \frac{\eta}{2m} \sum_{i=1}^m \|\nabla F_i(\hat{x}_i^t) - \nabla F_i(x_i^t)\|^2
\end{aligned} \tag{60}$$

$$\begin{aligned}
& \stackrel{(e)}{\leq} -\frac{\eta}{2} \left\| \frac{1}{m} \sum_{i=1}^m \nabla F_i(\hat{x}_i^t) \right\|^2 - \frac{\eta}{2} \left\| \frac{1}{m} \sum_{i=1}^m \nabla F_i(x_i^t) \right\|^2 \\
& \quad + \frac{\eta L^2}{2m} \sum_{i=1}^m \|w_i^t - w^k\|^2
\end{aligned} \tag{61}$$

$$\begin{aligned}
& = -\frac{\eta}{2} \left\| \frac{1}{m} \sum_{i=1}^m \nabla F_i(\hat{x}_i^t) \right\|^2 - \frac{\eta}{2} \left\| \frac{1}{m} \sum_{i=1}^m \nabla F_i(x_i^t) \right\|^2 \\
& \quad + \frac{\eta L^2}{2} V^t,
\end{aligned} \tag{62}$$

where (e) comes from Assumption 1. \square

Lemma B.5. *Suppose Assumptions 2 and 3 hold. For $t_p + 1 \leq t \leq v_p$, we have*

$$\begin{aligned}
& \mathbb{E}[V^t] \\
& \leq \lambda(K-1)(A_1+1) \sum_{\tau=t_p}^{t-1} \eta_\tau^2 \mathbb{E} \left[\left\| \frac{1}{m} \sum_{i=1}^m \nabla F_i(x_i^\tau) \right\|^2 \right]
\end{aligned} \tag{63}$$

$$\begin{aligned}
& + \sigma_G^2(K-1)(A_1+1) \sum_{\tau=t_p}^{t-1} \eta_\tau^2 + \frac{\sigma_w^2(K-1)}{B} \sum_{\tau=t_p}^{t-1} \eta_\tau^2.
\end{aligned} \tag{64}$$

Note that $V^{t_p} = 0$.

Proof. Note that $w^{t_p} = w_i^{t_p}$ for all $i \in [m]$. Thus, for $t_p + 1 \leq t \leq v_p$, we have

$$\begin{aligned} \|w_i^t - w^k\|^2 &= \left\| w_i^t - \sum_{\tau=t_p}^{t-1} \eta_\tau g_{i,1}^\tau - w^{t_p} - \sum_{\tau=t_p}^{t-1} \eta_\tau h^\tau \right\|^2 \\ &= \left\| \sum_{\tau=t_p}^{t-1} \eta_\tau g_{i,1}^\tau - \sum_{\tau=t_p}^{t-1} \eta_\tau h^\tau \right\|^2. \end{aligned} \quad (65)$$

Since

$$\frac{1}{m} \sum_{i=1}^m \sum_{\tau=t_p}^{t-1} \eta_\tau g_{i,1}^\tau = \sum_{\tau=t_p}^{t-1} \eta_\tau h^\tau. \quad (66)$$

Then we have

$$\frac{1}{m} \sum_{i=1}^m \|w_i^t - w^t\|^2 \quad (67)$$

$$= \frac{1}{m} \sum_{i=1}^m \left\| \sum_{\tau=t_p}^{t-1} \eta_\tau g_{i,1}^\tau - \sum_{\tau=t_p}^{t-1} \eta_\tau h^\tau \right\|^2 \quad (68)$$

$$= \frac{1}{m} \sum_{i=1}^m \left\| \sum_{\tau=t_p}^{t-1} \eta_\tau g_{i,1}^\tau \right\|^2 - \left\| \sum_{\tau=t_p}^{t-1} \eta_\tau h^\tau \right\|^2 \quad (69)$$

$$\leq \frac{1}{m} \sum_{i=1}^m \left\| \sum_{\tau=t_p}^{t-1} \eta_\tau g_{i,1}^\tau \right\|^2 \leq \frac{t-t_p}{m} \sum_{i=1}^m \sum_{\tau=t_p}^{t-1} \eta_\tau^2 \|g_{i,1}^\tau\|^2 \quad (70)$$

$$\leq \frac{K-1}{m} \sum_{i=1}^m \sum_{\tau=t_p}^{t-1} \eta_\tau^2 \|g_{i,1}^\tau\|^2. \quad (71)$$

Given $\{x_i^t\}_{i \in [m]}$, we have

$$\mathbb{E} \left[\frac{1}{m} \sum_{i=1}^m \|g_{i,1}^t\|^2 \right] = \frac{1}{m} \sum_{i=1}^m \mathbb{E} \left[\|g_{i,1}^t\|^2 \right] \quad (72)$$

$$\begin{aligned} &= \frac{1}{m} \sum_{i=1}^m \mathbb{E} \left[\|g_{i,1}^t - \nabla_w F_i(x_i^t)\|^2 \right] \\ &+ \frac{1}{m} \sum_{i=1}^m \|\nabla_w F_i(x_i^t)\|^2 \end{aligned} \quad (73)$$

$$\begin{aligned} &\leq \frac{1}{m} \sum_{i=1}^m \left[(A_1 + 1) \|\nabla F_i(x_i^t)\|^2 + \sigma_w^2 \right] \\ &+ \frac{1}{m} \sum_{i=1}^m \|\nabla F_i(x_i^t)\|^2 \end{aligned} \quad (74)$$

$$= \frac{A_1 + 1}{m} \sum_{i=1}^m \|\nabla F_i(x_i^t)\|^2 + \sigma_w^2. \quad (75)$$

where the expectation is taken with respect to the randomness in ξ^t . Thus, by the independence of $\xi^{(1)}, \xi^{(2)}, \dots, \xi^t$ and taking an unconditional expectation on both sides of (71), we have

$$\mathbb{E} [V^t] = (K-1) \sum_{\tau=t_p}^{t-1} \eta_\tau^2 \mathbb{E} \left[\mathbb{E} \left[\frac{1}{m} \sum_{i=1}^m \|g_{i,1}^\tau\|^2 \right] \right] \quad (76)$$

$$\leq (K-1)(A_1+1) \sum_{\tau=t_p}^{t-1} \eta_\tau^2 \mathbb{E} \left[\frac{1}{m} \sum_{i=1}^m \|\nabla F_i(x_i^\tau)\|^2 \right] \\ + (K-1)\sigma_w^2 \sum_{\tau=t_p}^{t-1} \eta_\tau^2 \quad (77)$$

$$\leq \lambda(K-1)(A_1+1) \sum_{\tau=t_p}^{t-1} \eta_\tau^2 \mathbb{E} \left[\left\| \frac{1}{m} \sum_{i=1}^m \nabla F_i(x_i^\tau) \right\|^2 \right] \\ + \sigma_G^2(K-1)(A_1+1) \sum_{\tau=t_p}^{t-1} \eta_\tau^2 + (K-1)\sigma_w^2 \sum_{\tau=t_p}^{t-1} \eta_\tau^2, \quad (78)$$

where the last inequality follows Assumption 3. \square

B.2 Proof of Theorem 3.5

Under Assumptions 1-3, given $\{x_i^t\}_{i \in [m]}$, it follows from Lemmas B.2-B.5 that

$$\mathbb{E} \left[\frac{1}{m} \sum_{i=1}^m F_i(\hat{x}_i^{t+1}) \right] - \frac{1}{m} \sum_{i=1}^m F_i(\hat{x}_i^t) \leq \\ - \frac{\eta}{2} \left\| \frac{1}{m} \sum_{i=1}^m F_i(\hat{x}_i^t) \right\|^2 - \frac{\eta}{2} \left\| \frac{1}{m} \sum_{i=1}^m F_i(x_i^t) \right\|^2 + \frac{\eta L^2}{2} V^t \\ + \frac{1}{2} \eta^2 L \lambda \left(\frac{A_1}{m} + A_2 + 1 \right) \left\| \frac{1}{m} \sum_{i=1}^m F_i(x_i^t) \right\|^2 \\ + \frac{1}{2} \eta^2 L \lambda \left\{ \left(\frac{A_1}{m} + A_2 + 1 \right) \sigma_G^2 + \frac{\sigma_w^2}{m} + \sigma_\beta^2 \right\}, \quad (79)$$

where the expectation is taken with respect to the randomness in ξ^t . Thus, taking the unconditional expectation on both sides of the equation above, we have

$$\mathbb{E} \left[\frac{1}{m} \sum_{i=1}^m F_i(\hat{x}_i^{t+1}) - \frac{1}{m} \sum_{i=1}^m F_i(\hat{x}_i^t) \right] \\ \leq - \frac{\eta}{2} \mathbb{E} \left[\left\| \frac{1}{m} \sum_{i=1}^m F_i(\hat{x}_i^t) \right\|^2 \right] - \frac{\eta}{2} \mathbb{E} \left[\left\| \frac{1}{m} \sum_{i=1}^m F_i(x_i^t) \right\|^2 \right] \\ + \frac{\eta L^2}{2} \mathbb{E} [V^t] \quad (80)$$

$$+ \frac{1}{2} \eta^2 L \lambda \left(\frac{A_1}{m} + A_2 + 1 \right) \mathbb{E} \left[\left\| \frac{1}{m} \sum_{i=1}^m F_i(x_i^t) \right\|^2 \right] \\ + \frac{1}{2} \eta^2 L \lambda \left\{ \left(\frac{A_1}{m} + A_2 + 1 \right) \sigma_G^2 + \frac{\sigma_w^2}{m} + \sigma_\beta^2 \right\}, \quad (81)$$

which implies that

$$\begin{aligned}
& \mathbb{E} \left[\frac{1}{m} \sum_{i=1}^m F_i(\hat{x}_i^{t_p+1}) - \frac{1}{m} \sum_{i=1}^m F_i(\hat{x}_i^{t_p}) \right] \\
&= \sum_{\tau=t_p}^{v_p} \mathbb{E} \left[\frac{1}{m} \sum_{i=1}^m F_i(\hat{x}_i^{\tau+1}) - \frac{1}{m} \sum_{i=1}^m F_i(\hat{x}_i^{\tau}) \right] \tag{82}
\end{aligned}$$

$$\begin{aligned}
&\leq -\frac{\eta}{2} \sum_{\tau=t_p}^{v_p} \mathbb{E} \left[\left\| \frac{1}{m} \sum_{i=1}^m F_i(\hat{x}_i^{\tau}) \right\|^2 \right] \\
&+ \frac{\eta}{2} \left\{ -1 + \eta L \lambda \left(\frac{A_1}{m} + A_2 + 1 \right) \right\} \\
&\sum_{\tau=t_p}^{v_p} \mathbb{E} \left[\left\| \frac{1}{m} \sum_{i=1}^m F_i(x_i^{\tau}) \right\|^2 \right] \tag{83}
\end{aligned}$$

$$\begin{aligned}
&+ \frac{\eta L^2}{2} \sum_{\tau=t_p}^{v_p} \mathbb{E}[V^{\tau}] \\
&+ \sum_{\tau=t_p}^{v_p} \frac{1}{2} \eta^2 L \lambda \left\{ \left(\frac{A_1}{m} + A_2 + 1 \right) \sigma_G^2 + \frac{\sigma_w^2}{m} + \sigma_{\beta}^2 \right\}. \tag{84}
\end{aligned}$$

By Lemma B.5, for all $t_p \leq \tau \leq v_p$, we have that

$$\mathbb{E}[V^{\tau}] \tag{85}$$

$$\begin{aligned}
&\leq \lambda \eta^2 (K-1) (A_1 + 1) \sum_{\tau=t_p}^{t-1} \mathbb{E} \left[\left\| \frac{1}{m} \sum_{i=1}^m \nabla F_i(x_i^{\tau}) \right\|^2 \right] \\
&+ \eta^2 \sigma_G^2 (K-1) (A_1 + 1) (\tau - t_p) + \eta^2 \sigma_w^2 (K-1) (\tau - t_p) \tag{86}
\end{aligned}$$

$$\begin{aligned}
&\leq \lambda \eta^2 (K-1) (A_1 + 1) \sum_{\tau=t_p}^{v_p} \mathbb{E} \left[\left\| \frac{1}{m} \sum_{i=1}^m \nabla F_i(x_i^{\tau}) \right\|^2 \right] \\
&+ \eta^2 \sigma_G^2 (K-1)^2 (A_1 + 1) + \eta^2 \sigma_w^2 (K-1)^2. \tag{87}
\end{aligned}$$

Therefore, we have

$$\begin{aligned}
&\frac{\eta L^2}{2} \sum_{\tau=t_p}^{v_p} \mathbb{E}[V^{\tau}] \\
&\leq \frac{1}{2} \lambda \eta^3 L^2 (K-1) K (A_1 + 1) \sum_{\tau=t_p}^{v_p} \mathbb{E} \left[\left\| \frac{1}{m} \sum_{i=1}^m \nabla F_i(x_i^{\tau}) \right\|^2 \right] \\
&+ \sum_{\tau=t_p}^{v_p} \frac{1}{2} \eta^3 L^2 \sigma_G^2 (K-1)^2 (A_1 + 1) + \sum_{\tau=t_p}^{v_p} \frac{\eta^3 L^2 \sigma_w^2 (K-1)^2}{2}. \tag{88}
\end{aligned}$$

Combined with (82), we have

$$\begin{aligned}
& \mathbb{E} \left[\frac{1}{m} \sum_{i=1}^m \nabla F_i(\hat{x}_i^{t_{p+1}}) - \frac{1}{m} \sum_{i=1}^m \nabla F_i(\hat{x}_i^{t_p}) \right] \\
& \leq -\frac{\eta}{2} \sum_{\tau=t_p}^{v_p} \mathbb{E} \left[\left\| \frac{1}{m} \sum_{i=1}^m \nabla F_i(\hat{x}_i^\tau) \right\|^2 \right] \\
& + \frac{\eta}{2} \left\{ -1 + \eta L \lambda \left(\frac{A_1}{m} + A_2 + 1 \right) + \right. \\
& \quad \left. \lambda \eta^2 L^2 (K-1) K (A_1 + 1) \right\} \sum_{\tau=t_p}^{v_p} \mathbb{E} \left[\left\| \frac{1}{m} \sum_{i=1}^m \nabla F_i(x_i^\tau) \right\|^2 \right] \\
& + \sum_{\tau=t_p}^{v_p} \frac{1}{2} \eta^2 L \lambda \left\{ \left(\frac{A_1}{m} + A_2 + 1 \right) \sigma_G^2 + \frac{\sigma_w^2}{m} + \sigma_\beta^2 \right\} \\
& + \sum_{\tau=t_p}^{v_p} \frac{1}{2} \eta^3 L^2 \sigma_G^2 (K-1)^2 (A_1 + 1) \\
& + \sum_{\tau=t_p}^{v_p} \frac{\eta^3 L^2 \sigma_w^2 (K-1)^2}{2}. \tag{89}
\end{aligned}$$

Due to

$$\begin{aligned}
& -1 + \eta L \lambda \left(\frac{A_1}{m} + A_2 + 1 \right) + \lambda \eta^2 L^2 (K-1) K (A_1 + 1) \\
& \leq 0, \tag{90}
\end{aligned}$$

which implies that

$$\begin{aligned}
& \mathbb{E} \left[\frac{1}{m} \sum_{i=1}^m \nabla F_i(x_i^{t_{p+1}}) - \frac{1}{m} \sum_{i=1}^m \nabla F_i(x_i^{t_p}) \right] \\
& \leq -\frac{\eta}{2} \sum_{\tau=t_p}^{v_p} \mathbb{E} \left[\left\| \frac{1}{m} \sum_{i=1}^m \nabla F_i(\hat{x}_i^\tau) \right\|^2 \right] \\
& + \sum_{\tau=t_p}^{v_p} \frac{1}{2} \eta^2 L \lambda \left\{ \left(\frac{A_1}{m} + A_2 + 1 \right) \sigma_G^2 + \frac{\sigma_w^2}{m} + \sigma_\beta^2 \right\} \\
& + \sum_{\tau=t_p}^{v_p} \frac{1}{2} \eta^3 L^2 \sigma_G^2 (K-1)^2 (A_1 + 1) \\
& + \sum_{\tau=t_p}^{v_p} \frac{\eta^3 L^2 \sigma_w^2 (K-1)^2}{2}. \tag{91}
\end{aligned}$$

Since we have assumed that $T = t_{\bar{p}}$ for some $\bar{p} \in \mathbb{N}^+$, we further have

$$\begin{aligned} & \frac{1}{T} \mathbb{E} \left[\left(\frac{1}{m} \sum_{i=1}^m \nabla F_i (\hat{x}_i^T) - f^* \right) \right. \\ & \quad \left. - \left(\frac{1}{m} \sum_{i=1}^m \nabla F_i (\hat{x}_i^0) - f^* \right) \right] \end{aligned} \quad (92)$$

$$= \frac{1}{T} \mathbb{E} \left[\frac{1}{m} \sum_{i=1}^m \nabla F_i (\hat{x}_i^t) - \frac{1}{m} \sum_{i=1}^m \nabla F_i (\hat{x}_i^0) \right] \quad (93)$$

$$= \frac{1}{T} \sum_{p=0}^{\bar{p}-1} \mathbb{E} \left[\frac{1}{m} \sum_{i=1}^m \nabla F_i (\hat{x}_i^{t_{p+1}}) - \frac{1}{m} \sum_{i=1}^m \nabla F_i (\hat{x}_i^{t_p}) \right] \quad (94)$$

$$\begin{aligned} & \leq -\frac{\eta}{2K} \sum_{p=0}^{\bar{p}-1} \sum_{\tau=t_p}^{v_p} \mathbb{E} \left[\left\| \frac{1}{m} \sum_{i=1}^m \nabla F_i (\hat{x}_i^t) \right\|^2 \right] \\ & \quad + \frac{1}{T} \sum_{p=0}^{\bar{p}-1} \sum_{\tau=t_p}^{v_p} \frac{1}{2} \eta^2 L \lambda \left\{ \left(\frac{A_1}{m} + A_2 + 1 \right) \sigma_G^2 + \frac{\sigma_w^2}{m} + \sigma_\beta^2 \right\} \end{aligned} \quad (95)$$

$$\begin{aligned} & \quad + \frac{1}{T} \sum_{p=0}^{\bar{p}-1} \sum_{\tau=t_p}^{v_p} \frac{1}{2} \eta^3 L^2 \sigma_G^2 (K-1)^2 (A_1 + 1) \\ & \quad + \frac{1}{T} \sum_{p=0}^{\bar{p}-1} \sum_{\tau=t_p}^{v_p} \frac{\eta^3 L^2 \sigma_w^2 (\tau-1)^2}{2} \end{aligned} \quad (96)$$

$$\begin{aligned} & = -\frac{\eta}{2T} \sum_{t=0}^{T-1} \mathbb{E} \left[\left\| \frac{1}{m} \sum_{i=1}^m \nabla F_i (\hat{x}_i^t) \right\|^2 \right] \\ & \quad + \frac{1}{2} \eta^2 L \lambda \left\{ \left(\frac{A_1}{m} + A_2 + 1 \right) \sigma_G^2 + \frac{\sigma_w^2}{m} + \sigma_\beta^2 \right\} \end{aligned} \quad (97)$$

$$+ \frac{1}{2} \eta^3 L^2 \sigma_G^2 (K-1)^2 (A_1 + 1) + \frac{\eta^3 L^2 \sigma_w^2 (K-1)^2}{2}. \quad (98)$$

We can conclude that

$$\begin{aligned} & \frac{1}{T} \sum_{t=0}^{T-1} \mathbb{E} \left[\left\| \frac{1}{m} \sum_{i=1}^m \nabla F_i (\hat{x}_i^t) \right\|^2 \right] \\ & \leq \frac{2 \mathbb{E} \left[\frac{1}{m} \sum_{i=1}^m \nabla F_i (\hat{x}_i^0) - f^* \right]}{\eta T} \\ & \quad + \eta L \lambda \left\{ \left(\frac{A_1}{m} + A_2 + 1 \right) \sigma_G^2 + \frac{\sigma_w^2}{m} + \sigma_\beta^2 \right\} \\ & \quad + \eta^2 L^2 \sigma_G^2 (K-1)^2 (A_1 + 1) + \eta^2 L^2 \sigma_w^2 (K-1)^2. \end{aligned} \quad (99)$$

C Additional Experiment Results and Experiment Details

C.1 Toy examples

In this subsection, we present the comprehensive comparison results illustrated in Figure 2 of the main paper, showcasing various levels of client cooperation, as depicted in Figure 6. The overall test accuracy performance is further demonstrated in Figure 7.

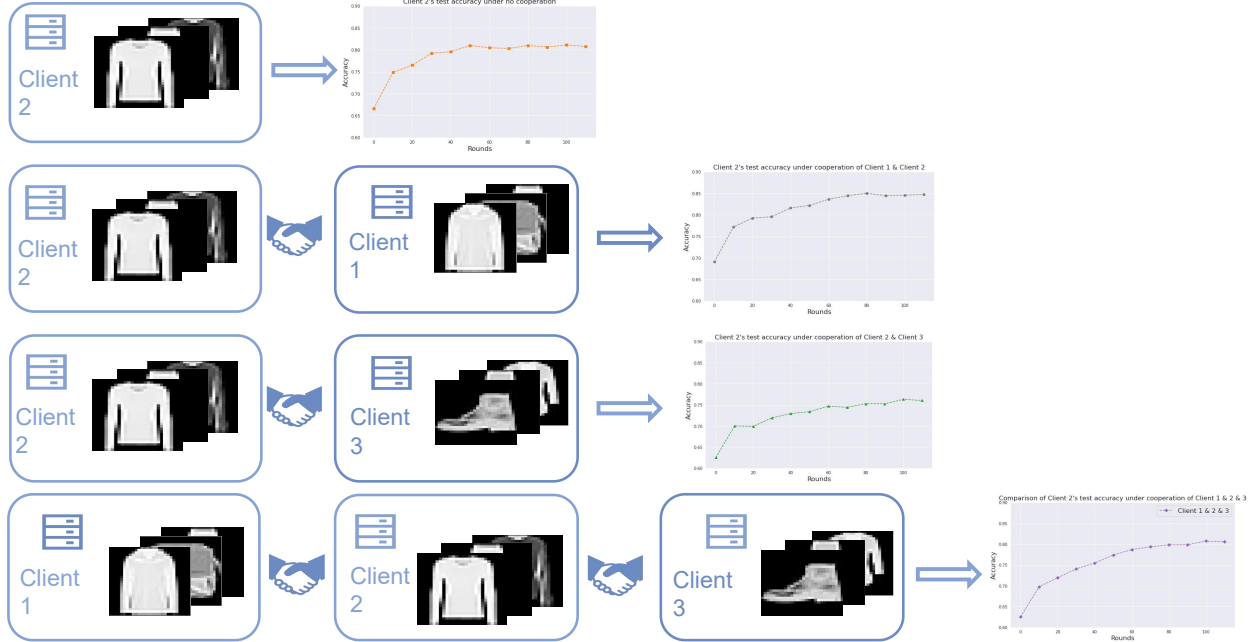


Figure 6: Illustration of different cooperation methods.

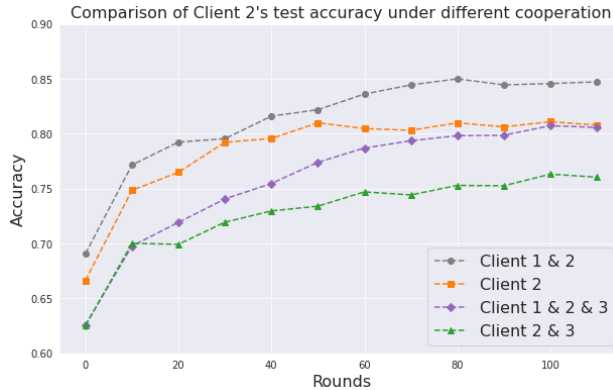


Figure 7: The test accuracy of different cooperation of clients on FashionMNIST.

C.2 Experimental Environment

For our experiments, we use NVIDIA GeForce RTX 3090 GPUs. Each simulation trail with 500 communication rounds and three random seeds.

C.3 Experiment setup

Training Settings. We maintain the same experimental settings for all baselines, conducting 500 communication rounds with 100 clients. The client sampling ratio is set to 0.1 for the baselines, while in DFL, when implementing sampling methods like gossip, each client communicates with 10 neighbors. The batch size is 64 for FEMNIST and 128 for CIFAR. The local epochs per round are set to 5 for all baselines, while the local fine-tune epoch is set to 1 by default. We employ SGD with momentum as the base optimizer with a learning rate of $\eta = 0.01$ and a local momentum of 0.9.

Setup for FashionMNIST, CIFAR-10 and CIFAR-100. To evaluate the performance of our algorithm AFIND+, we train a two-layer CNN on the non-iid FashionMNIST and four-layer CNN on CIFAR-10 datasets, and a ResNet-18 on the non-iid CIFAR-100 dataset, respectively.

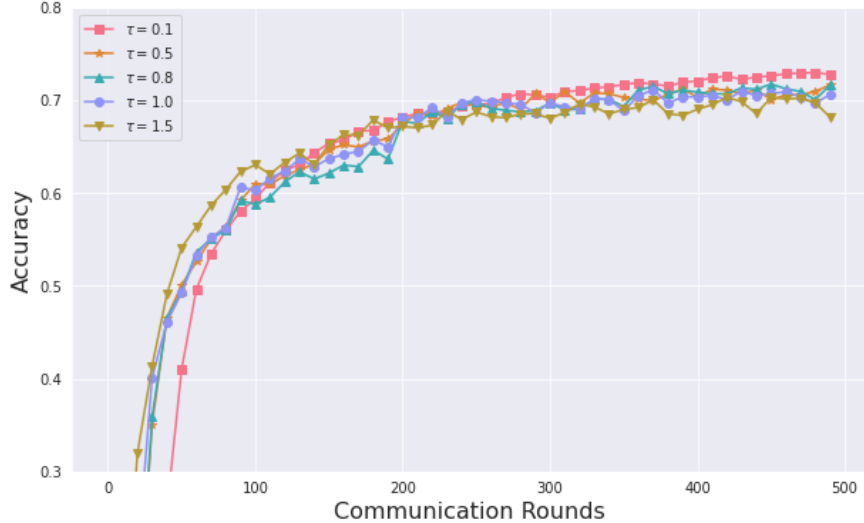


Figure 8: Ablation study for τ on CIFAR-10.

Unless specifically mentioned otherwise, our studies use the following protocol: the default non-IID is from Dirichlet with a parameter of $\alpha = 0.5$, the server chooses 10% clients according to sampling strategy from the total of $m = 100$ clients, and each is trained for $T = 500$ communication rounds with $K = 5$ local epochs.

All sampling algorithms use FedAvg-FT as the backbone. We compare our AFIND+ with Gossip sampling, PENS, and FederiCo on different datasets and different settings.

Setup for LEAF. To test our algorithm’s efficiency on diverse real datasets, we use the non-IID FEMNIST dataset in LEAF, as given in [36]. All baselines use a 4-layer CNN with a learning rate of 0.1, batch size of 32, sample ratio of 10% and communication round of $T = 500$. The reported results are averaged over three runs with different random seeds.

C.4 Additional Experimental Results

Ablation study for τ of AFINE+ on CIFAR-10. Figure 8 shows the convergence performance of AFIND+ on the CIFAR-10 dataset with $\alpha = 0.1$, under different global thresholds, specifically $\tau = 0.1, 0.5, 0.8, 1.0, 1.5$. Different thresholds lead to different client participation behaviors for DFL, demonstrating the stability of our algorithm to the hyperparameter τ . Additionally, a smaller $\tau = 0.2$ tends to result in better performance, but the requirement of training rounds for convergence is larger. In contrast, a larger τ leads to faster convergence, but the accuracy is slightly poorer since the participation number of clients is small when the threshold is large.

Ablation study for network topologies. Table 3 shows the performance of different sampling methods when applied to a partially connected network topology, in which each client randomly connects to half of the other clients. As the network typology becomes more challenging (from full connection to partial connection), the advantage of AFIND+ becomes more significant than other baselines because AFINE+ can adaptively adjust each client’s sampling numbers, enabling flexible neighbor connections.

Privacy evaluation. We also evaluate AFIND+ under privacy preservation. Following [57], we insert Gaussian noise into the intermediate regularization variable δ with noise standard deviation $\sigma_2 : \tilde{\sigma}_i \leftarrow \sigma_i + \frac{1}{L} \mathcal{N}(0, \sigma_2^2 C_0^2 I)$, where L is the batch size, σ_2 is the noise parameter, C_2 is the clipping constant. The result is shown in Table 4. With $\sigma_2 \leq 5$, AFIND+ shows only marginal reductions without significant performance degradation. However, higher values of σ_2 risk compromising performance. This suggests that our approach is compatible with a specific threshold of privacy preservation.

Table 3: Performance of sampling algorithms on the **partially connected network**. In the partially connected network, each client is randomly connected to others. In the full connection network typology (Table 1), each client is connected to all others.

Algorithm	CIFAR-10		CIFAR-100	
	$\alpha = 0.1$	$c = 5$	$\alpha = 0.1$	$c = 10$
Gossip	51.35±1.76	68.12±2.47	49.61±1.74	58.64±1.38
PENS	53.78±1.32	70.46±1.57	51.24±1.53	61.01±1.94
FedeRiCo	55.85±1.15	71.58±1.93	53.21±1.64	63.41±1.57
AFIND+	65.24±2.12	76.21±2.12	58.87±2.18	66.85±2.15

Table 4: Performance of AFIND+ under **differential privacy noise**. Insert Gaussian noise into the intermediate regularization variable δ with noise standard deviation σ_2 .

noise σ_2	CIFAR-10		CIFAR-100	
	$\alpha = 0.1$	$c = 5$	$\alpha = 0.1$	$c = 10$
0	71.89±0.06	80.36±0.32	62.11±1.82	71.07±1.02
2	70.61±0.14	79.67±1.34	61.07±0.40	70.82±1.51
5	69.94±1.42	78.85±0.62	60.72±0.16	68.23±1.23
10	67.07±0.42	76.11±1.74	58.41±1.52	66.05±0.87
50	64.24±1.56	73.92±1.08	55.86±1.12	63.20±1.18